Polyamine depletion limits progression of acute leukaemia

Weiman Gao[1,2]*, Mawar Karsa[1,2]*, Lin Xiao[1,2], Dayna Spurling[1], Ayu Karsa[1], Emma Ronca[1], Angelika Bongers[1], Xinyi Guo[1], Chelsea Mayoh[1,2], Mujahid Azfar[3], Steven H L Verhelst[4], Katsunori Tanaka[5,6], Laurence C Cheung[7,8,9], Rishi S Kotecha[7,8,10,11] Richard B Lock[1,2], Mark R Burns[12], Peter Vangheluwe[3], Murray D Norris[1,2], Michelle Haber[1,2], Klaartje Somers[1,2$]

[1] Children's Cancer Institute, Lowy Cancer Research Centre, UNSW Sydney, Sydney, NSW, Australia

[2] School of Clinical Medicine, UNSW Medicine & Health, UNSW Centre for Childhood Cancer research, UNSW Sydney, Sydney, NSW, Australia

[3] Laboratory of Cellular Transport Systems, Department of Cellular and Molecular Medicine, KU Leuven, Leuven, Belgium

[4] Laboratory of Chemical Biology, Department of Cellular and Molecular Medicine, KU Leuven, Leuven, Belgium

[5] Department of Chemical Science and Engineering, School of Materials and Chemical Technology, Tokyo Institute of Technology, 2-12-1 Ookayama, Meguro-ku, Tokyo, Japan

[6] Biofunctional Synthetic Chemistry Laboratory, RIKEN Cluster for Pioneering Research, 2-1 Hirosawa, Wako-shi, Saitama, Japan

[7] Leukaemia Translational Research Laboratory, Telethon Kids Cancer Centre, Telethon Kids Institute, Perth, WA, Australia

[8] Curtin Medical School, Curtin University, Perth, WA, Australia

[9] Curtin Health Innovation Research Institute, Curtin University, Perth, WA, Australia

[10] Department of Clinical Haematology, Oncology, Blood and Marrow Transplantation, Perth Children's Hospital, Perth, WA, Australia

[11] Division of Paediatrics, School of Medicine, University of Western Australia, Perth, WA, Australia

[12] Aminex Therapeutics, Aminex Therapeutics Inc., Kirkland, WA, USA

* Shared first authors

$ Corresponding author: Klaartje Somers, Children's Cancer Institute, Lowy Cancer Research Centre, UNSW Sydney, ksomers@ccia.org.au

Keywords: Acute leukaemia, polyamines, polyamine depletion, DFMO, polyamine transport

Abbreviations: ALL, acute lymphoblastic leukaemia; AML, acute myeloid leukaemia; AraC, cytarabine; BDP, BODIPY; DNR, daunorubicin; DFMO, difluoromethylornithine; ODC1, ornithine decarboxylase 1; MPAL, mixed phenotype acute leukaemia; PUT, putrescine; SPD, spermidine; SPM, spermine;

Article category: Cancer Therapy and Prevention

Novelty and impact: We demonstrated that acute leukaemia cell growth and survival are dependent on elevated intracellular polyamine levels and that polyamine depletion by simultaneous inhibition of cellular polyamine synthesis and polyamine uptake from the environment, kills these cells. Polyamine depletion delays progression in animal models of aggressive leukaemia with poor outcome, providing support for its use as a potential treatment strategy for acute leukaemia worthy of further investigation.

Abstract

Cancer cells are addicted to polyamines, polycations essential for cellular function. While dual targeting of cellular polyamine biosynthesis and polyamine uptake is under clinical investigation in solid cancers, preclinical and clinical studies into its potential in haematological malignancies are lacking. Here we investigated the preclinical efficacy of polyamine depletion in acute leukaemia. The polyamine biosynthesis inhibitor difluoromethylornithine (DFMO) inhibited growth of a molecularly diverse panel of acute leukaemia cell lines, while non-malignant cells were unaffected. Responsiveness to DFMO was linked to decreased levels of its molecular target, the rate-limiting polyamine biosynthesis enzyme ODC1, and of the polyamine transporters ATP13A2 and ATP13A3. DFMO increased polyamine uptake and upregulated expression of polyamine transporters in acute leukaemia cells, a compensatory effect abolished by treatment with the polyamine transport inhibitor AMXT 1501. This drug, currently in a phase 1 clinical trial in solid tumours in combination with DFMO, potentiated the inhibitory effects of DFMO, and their combination synergistically inhibited the growth of acute leukaemia cell lines by inducing apoptosis. DFMO and AMXT 1501 limited disease progression in highly aggressive xenograft models of infant *KMT2A*-rearranged leukaemia, even when treatment was initiated at high disease burden. Increased expression of c-MYC was associated with enhanced sensitivity to the combination of DFMO and AMXT 1501, suggesting this oncoprotein as a potential predictive marker of response to the drug combination. In

conclusion, targeting polyamine biosynthesis and polyamine uptake limits disease progression in models of acute leukaemia, supporting further preclinical and clinical investigation into this approach for acute leukaemia.

Introduction

Less than three out of ten adults suffering from acute leukaemia survive five years from diagnosis [1]. For children with acute leukaemia, survival rates have increased dramatically over the past few decades, however, one out of ten patients with acute lymphoblastic leukaemia (ALL) and three out of ten with acute myeloid leukaemia (AML) still relapse, of whom more than half will succumb to the disease [2]. Moreover, most survivors will suffer from detrimental long-term health effects that significantly decrease their quality of life [1,2]. There remains a high unmet need to develop novel, more targeted treatment options for acute leukaemia that are effective for patients who do not respond to established therapy and that do not cause harmful side effects associated with current standard of care drugs.

Targeting the addiction of cancer cells to polyamines, small polycations that support essential cellular processes upon which cancer cells are reliant for their rapid growth and function, has been under investigation as a chemopreventative and cancer treatment strategy for several decades [3,4]. While difluoromethylornithine (DFMO), a well-characterised drug that blocks the main rate-limiting enzyme of cellular polyamine biosynthesis ornithine decarboxylase 1 (ODC1), was recently approved as a maintenance therapy in patients in remission for high-risk neuroblastoma [5,6], agents targeting this pathway have in general failed to achieve major clinical successes as a therapeutic strategy [7-10]. It was recently discovered that upon inhibition of polyamine biosynthesis, solid cancer cells can upregulate uptake of polyamines from the extracellular milieu to compensate for polyamine depletion [11-14], inspiring the development of novel agents targeting polyamine transport [11-14]. We previously demonstrated that a newly developed transport inhibitor, AMXT 1501, potentiated the cancer inhibitory effects of DFMO) [12,13]. Simultaneous inhibition of polyamine biosynthesis and uptake, by combining DFMO and AMXT 1501, induced impressive delays in progression in models of solid cancers, including high-risk neuroblastoma and a fatal brain cancer in children, diffuse intrinsic pontine glioma (DIPG) [12,13]. Based on these preclinical data, the combination of DFMO and AMXT 1501 was investigated in a completed first in-human clinical trial in solid cancers (NCT03536728) and is currently in a follow-up Phase 1B/2A trial (NCT05500508).

Patients with leukaemia also exhibit elevated polyamine levels and enhanced activities of enzymes involved in polyamine biosynthesis [15-18]. However, the few clinical studies that

were performed in the 1980s testing the efficacy of polyamine biosynthesis inhibition drugs including DFMO for leukaemia, yielded mediocre results at best [9,10]. It is not understood why polyamine biosynthesis inhibition failed in acute leukaemia. To our knowledge, the therapeutic potential of targeting polyamine uptake combined with polyamine biosynthesis inhibition has so far not been studied in leukaemia cells and may offer a way forward to potentiate polyamine depletion strategies for the treatment of this disease.

Here we demonstrate for the first time that targeting polyamine biosynthesis in acute leukaemia cells by treatment with DFMO boosts polyamine uptake from the external environment, an effect abrogated by the transport inhibitor AMXT 1501. We show that simultaneous inhibition of polyamine synthesis and uptake synergistically kills leukaemia cells by inducing apoptosis and delays leukaemia progression in highly aggressive and treatment-resistant xenograft models, thereby presenting as a therapeutic strategy worthy of further investigation for leukaemia.

Materials and Methods

Cell lines and cell culture

The panel of cell lines used in this study is described in Supplementary Table 1. All cell lines were authenticated by STR-profiling within the last three years and all experiments were performed with mycoplasma-free cells. Short-term culture patient-derived cell lines, PER-485, PER-494, PER-703, PER-784, PER-785, PER-826 and PER-910 were cultured in RPMI (Thermo Fisher Scientific) with the addition of 20% (v/v) fetal bovine serum (Thermo Trace). The other leukaemia cell lines were grown in RPMI supplemented with 10% (v/v) fetal bovine serum. Culture medium for suspension cells was additionally supplemented with 2 mM L-glutamine, MEM Non-Essential Amino Acids and MEM Sodium Pyruvate Solution, all purchased from Invitrogen Life Technologies. All cells were maintained by passaging every 2-3 days and reseeding at a cell density of approximately 1-2 x 10^5 cells/ mL. The adherent MRC-5 cell line was cultured in alpha-MEM (Thermo Fisher Scientific) with 10% (v/v) fetal bovine serum. When cells reached 70-80% confluence, they were split 1:5-1:10 twice a week using trypsin (0.25% (w/v) in Hank's solution) (Invitrogen Life Technologies) for detachment. Experiments involving the addition of exogenous polyamines in culture media containing foetal bovine serum were performed in the presence of 1 mM aminoguanidine (Sigma-Aldrich).

Reagents

Polyamines putrescine dihydrochloride (P7505), spermidine (S2626) and spermine (3256) were purchased from Sigma-Aldrich. All polyamines were dissolved in 0.1 M MOPS-KOH

(pH 7.0). DFMO was kindly provided by Prof. Patrick M. Woster, Medical University of South Carolina. AMXT 1501 dicaprate was kindly provided by Aminex Therapeutics.

Cell-based assays

Drug cytotoxicity was assessed in resazurin reduction-based viability assays as previously described [19,20]. Viable cell counts were obtained in trypan blue exclusion assays. Synergy studies were performed in 6x6 matrix assays and synergy was scored according to the Bliss Independence model and visualised through Combenefit as previously described [21,22]. Synergy was evaluated at 25 different drug combinations with a positive Bliss score at each data point indicating synergy at that combination of drug concentrations. A Bliss sum was calculated for each cell line by adding up the Bliss scores at all drug combinations (up to 20 mM DFMO). The percentage of apoptotic cells was determined by staining cells with Annexin V and 7-Aminoactinomycin D (7-AAD) (BD Biosciences) followed by flow cytometry detection as previously described [19].

Immunoblotting

Protein analysis and immunoblotting were performed as previously described [23]. The following primary antibodies were used: anti-β-ACTIN (Sigma-Aldrich A2066), anti-GAPDH (Sigma, G8795), anti-CASPASE-3 (Cell Signaling Technologies, 14220S), anti-cleaved CASPASE-3 (Cell Signaling Technologies, 9664S), anti-ODC1 (Abcam, ab97395), anti-AMD1 (Proteintech, 11052-1-AP), anti-SLC3A2 (BioRad, VPA00372), anti-ATP13A2 (Sigma-Aldrich, A3361) and anti-ATP13A3 (Sigma-Aldrich, HPA029471) antibodies.

Polyamine-RED staining

Polyamine-RED was synthesised and kindly provided by Funakoshi Co. Ltd. Leukaemia cells were seeded, treated with 0.5 mM DFMO and harvested after 72 hours of treatment. Cells were collected and washed once with cold phosphate-buffered saline (PBS), followed by staining with 100 µL of 10 µM PolyamineRED in FACS buffer for 10 minutes. Samples were analysed by flow cytometry with a BD LSRFortessa™ (BD Biosciences).

BODIPY-polyamine uptake assays

Polyamine-BODIPY uptake was measured by flow cytometry as previously described [24]. For uptake assays involving AMXT 1501, cells were pre-treated overnight, and 500 nM fluorescently labelled polyamines were added at 37 °C for 30 minutes in the presence or absence of 1 mM aminoguanidine. The amount of polyamine being taken up into the cells was measured by flow cytometry using a BD FACSCanto™ (BD Biosciences). The level of polyamine uptake was represented by the ratio between the geometric mean fluorescence

intensity (Geo MFI) of cells after addition of polyamine-BODIPY and the Geo MFI of unstained (absence of polyamine-BODIPY) cells.

Radio-labelled polyamine uptake assays

^{3}H-Spermidine Trihydrochloride (NET522001MC), purchased from Perkin Elmer, and ^{3}H-Putrescine Dihydrochloride (ART-0279-1mCi), obtained from American Radiolabelled Chemicals, were added to cells at 0.1-0.2 µCi and incubated at 37 ºC for 60-90 minutes in the presence or absence of of 1 mM aminoguanidine. The reaction was stopped by rapid dilution with 1 mL ice-cold PBS followed by filtering the leukaemia cell suspension through glass fibre filters and washing once with 2 mL 50 µM cold putrescine or spermidine, then twice with Tris-buffered saline by vacuum filtration. The filters were air-dried, then transferred to scintillation vials with Ultima Gold liquid scintillation cocktail. ^{3}H radioactivity in each vial was measured by scintillation counting and normalised to cell number per mL.

Quantitative reverse transcription polymerase chain reaction (RT-PCR)

Expression levels of *ODC1* and *AMD1* were determined by quantitative RT-PCR as previously described [25]. The following primer sequences were used: *ODC1* FW primer: GGGCTGAGGTTGGTTTCA; *ODC1* REV primer: AACGCTGGGTTGATTACGC. *AMD1* FW primer: ACCACCTTGTTTGTTAATCAGAGTT; *AMD1* REV primer: ACCTTCAATCTTCTGGG GCG.

Animal experiments

All animal experiments were approved by the University of New South Wales Animal Care and Ethics Committee according to the Animal Research Act 1985, and the Australian Code of Practice for Care and Use of Animals for Scientific Purposes. Efficacy studies in the cell line xenograft and patient-derived xenograft (PDX) models were performed as previously described [20,23,26,27]. Event-free survival (EFS) was calculated as the days from treatment initiation until mice became moribund (i.e., reached a total score of 3 in body condition scoring based on coat condition, activity and body weight) (PER-485 model) or until the percentage of human CD45^{+} (%huCD45^{+}) cells reached 25% in peripheral blood (MLL-3 PDX model). Applied drug doses were determined based on maximally tolerated dose studies and previously performed efficacy studies in solid cancer models [12,28]. DFMO (1%) was added into drinking water until endpoint was reached. AMXT 1501 dicaprate salt (1.25 mg/kg free base content) was subcutaneously injected daily for 17 days. For the combination arm, DFMO and AMXT 1501 were administered according to their individual regimens. To evaluate interactions between drugs *in vivo*, Therapeutic Enhancement was defined if the EFS of mice treated with the drug combination was significantly greater than the EFS induced by each single agent as determined by Gehan-Wilcoxon [20,29].

Gene expression and survival analyses

Normalised RPKM (reads per kilobase million mapped read) counts from RNA sequencing data were extracted and compiled for samples in the Target II B-ALL (n=203, www.cbioportal.org) and TCGA AML (n=173, www.cbioportal.org) databases. Microarray data from the MILE study (N=2004, GSE13159) were obtained through the R2 database (https://r2.amc.nl). Expression levels of polyamine transporters were evaluated across haematological cancer cell lines in the BROAD Cancer Cell line database (n=135, GSE36133, www.cbioportal.org). As a measure for polyamine biosynthesis activity, a polyamine biosynthesis score was generated for each sample based on calculating a weighted average of expression decile for the biosynthetic genes [12]. All polyamine pathway genes of interest received a score ranging from 1 to 10 based on the normalised RPKM counts. A higher score corresponds to higher expression of biosynthetic genes; a score of 10 indicates the highest expression decile, while a score of 1 represents the lowest expression decile. The cumulative polyamine biosynthesis scores were computed by summing the scores for each individual gene, with a greater score reflecting elevated levels of polyamine synthesis activity within the cell. For survival analyses, patients were dichotomised based on the upper quartile (UQ) gene expression level or polyamine biosynthesis score level, and log-rank tests were performed to compare survival of high and low expression/score groups.

Statistical analyses

GraphPad Prism 9 (GraphPad software) was used for all analyses. Comparisons of variables between groups were performed as indicated in individual figure legends. In general, one sample t-tests or Student's t-tests were used to assess statistical significance of differences in measurements between two groups. One-way ANOVA with Tukey's correction for multiple comparisons was employed when analysing significance involving three or more groups. Pearson analysis was used to determine the correlation between two variables. Two-way ANOVA was employed to assess whether there were significant differences between groups formed by the combination of two variables. P-values less than 0.05 were considered statistically significant.

Results

Heightened activity of the polyamine biosynthesis pathway is predictive of inferior outcome in acute leukaemia

We first evaluated the activity of the polyamine biosynthesis pathway in patients with acute leukaemia by comparing the expression levels of the gene encoding the main rate-

limiting enzyme of polyamine biosynthesis, *ODC1* (Fig. 1A), as well as of other polyamine biosynthetic genes (*AMD1*, *SRM*, *SMS*), between patients with acute leukaemia and healthy controls in the MILE study database. As a measure for polyamine biosynthesis activity, a combined polyamine biosynthesis score was generated for all bone marrow mononuclear cell samples in the database with a higher score corresponding to a higher combined expression of biosynthetic genes [12]. Polyamine biosynthesis scores of samples from patients with B-cell ALL (B-ALL), T-cell ALL (T-ALL) and AML were significantly higher than those of healthy controls (Fig. 1B), confirming heightened activity of the polyamine biosynthesis pathway in acute leukaemia. Furthermore, when analysing the prognostic relevance of *ODC1* expression in ALL and AML patient datasets (Target I B-ALL, TCGA AML), high *ODC1* expression was found to be associated with worse overall survival in patients with ALL and AML (Fig. 1C, 1D), suggesting a biological role for heightened polyamine biosynthesis in acute leukaemia progression.

Targeting polyamine biosynthesis inhibits acute leukaemia cell growth and induces apoptosis

To further investigate the dependency of acute leukaemia cells on polyamine biosynthesis, we next assessed whether inhibition of polyamine synthesis by DFMO impacted cell viability. We selected three cell lines representative of different acute leukaemia subtypes, namely PER-485, representing infant *KMT2A*-rearranged mixed phenotype acute leukaemia (MPAL) [30]; CEM/C1, established from a patient with aggressive T-ALL; and Reh, a B-ALL cell line characterised by a *t*(12;21) translocation, the most common chromosomal rearrangement in childhood B-ALL. DFMO inhibited the viability and growth of all three leukaemia cell lines in a dose- and time-dependent fashion as assessed in trypan blue exclusion assays (Fig. 1E). In all three cell lines, 5 mM DFMO significantly limited leukaemia growth, an effect seen as early as three days after starting treatment. The observed inhibitory effects by DFMO were reversible by adding exogenous polyamines to the culture medium, providing evidence that the growth inhibition induced by DFMO treatment was indeed mediated through polyamine depletion (Fig. 1E). As exogenously added spermidine and spermine are substrates of bovine amine oxidases present in foetal bovine serum added to culture medium, which can result in polyamine degradation and the potential generation of cytotoxic byproducts, these studies were executed in the presence of aminoguanidine, a well-established inhibitor of amine oxidases, as previously established [31,32]. Further confirming the specific polyamine-depleting effect of DFMO in acute leukaemia cells, staining with the polyamine dye polyamine RED demonstrated a reduction in intracellular polyamine levels in DFMO-treated PER-485 cells (Supplementary Figure 1).

DFMO treatment caused a dose-dependent increase in the percentage of cells staining positive for Annexin V (marker of apoptosis), indicating that the drug induced apoptosis, an effect most pronounced in PER-485 and CEM/C1 cells (Fig. 1F). In all three cell lines, 5 mM DFMO significantly increased the population of apoptotic cells within three days of treatment (Fig. 1F). Consistent with the live cell count findings (Fig. 1E), addition of exogenous polyamines to the culture medium prevented apoptosis, demonstrating that polyamine depletion by DFMO was responsible for induction of apoptosis (Fig. 1F). Increased cleaved CASPASE-3 levels were shown in leukaemia cells treated with DFMO, further confirming induction of apoptosis (Fig. 1G).

Targeting polyamine synthesis inhibits growth in a molecularly and immunophenotypically diverse panel of acute leukaemia cells

Acute leukaemia encompasses a highly diverse collection of blood cancers, with numerous different leukaemogenic drivers and originating from progenitor cells of distinct lineages (e.g., myeloid versus lymphoid) and developmental state. To evaluate whether polyamine biosynthesis is important for cell survival and growth in different acute leukaemia subtypes, we assessed the effects of DFMO on cell growth in a large and diverse panel of cell lines (n=22) comprising of different immunophenotypes (B-ALL, T-ALL, AML, MPAL) and leukaemogenic drivers (e.g., *KMT2A* rearrangement, *CALM-AF10* translocation, *t*(11;19)) (Supplementary Table 1). We found that treatment with 2 mM DFMO for up to six days significantly inhibited growth of all leukaemia cell lines included in the panel, including highly aggressive, chemotherapy-resistant subtypes that are known to have poor outcomes (Fig. 2A). In contrast, DFMO did not impact the growth of the non-malignant lung fibroblast cell line MRC-5 (Fig. 2A). Immunoblotting for cleaved CASPASE-3 confirmed induction of apoptosis across different leukaemia subtypes (Fig. 2B).

Sensitivity to DFMO is associated with higher proliferation rate and decreased ODC1 expression

While DFMO significantly delayed cell growth in all 21 acute leukaemia cell lines included in the panel, we observed variability in responsiveness. For example, for Reh, treatment with DFMO abolished any cell growth, while for 697, a growth inhibition of 20% was achieved after 6 days of treatment (Fig. 2A). To understand the determinants of responsiveness to DFMO, response data were analysed with two different methods. In one approach, the response data of the entire leukaemia cell line panel were utilised in correlation analyses and through comparing parameters within two subgroups defined based on achieved % growth inhibition, i.e., *highly DFMO-sensitive* cells versus *less DFMO-sensitive* cells (Supplementary Figure 2). In a second, more reductive approach, characteristics of the two cell lines on opposite ends of the DFMO sensitivity spectrum

were compared, namely the PER-485 cells, being the most sensitive cell line to DFMO, and 697 cells, the least DFMO-responsive leukaemia cells within the panel (Supplementary Figure 2A).

We observed that *highly DFMO-sensitive* leukaemia cell lines exhibited a significantly shortened doubling time compared to *DFMO-sensitive* cells (Fig. 2C), consistent with prior findings linking hyperactivity of the polyamine pathway to solid tumour aggressiveness [33-36]. This finding is in line with faster growing leukaemia cells being more dependent on polyamines and thus more sensitive to inhibition of the polyamine biosynthesis pathway. Higher responsiveness to DFMO was not associated with a specific leukaemia subtype (Supplementary Figure 3).

Whether ODC1 expression level impacts responsiveness to DFMO has been a topic of debate. It was previously demonstrated that neuroblastoma cell lines that expressed higher levels of MYCN, which induces expression of ODC1, were more sensitive to DFMO [37]. This seemingly contrasts with a study in pancreatic cancer cell lines that found that reduced ODC1 levels translated into a higher responsiveness to DFMO, as less drug is needed to inhibit the protein [38]. Within our acute leukaemia cell line panel, a similar trend was observed as for the pancreatic cancer cells, with higher ODC1 expression being associated with diminished responsiveness to DFMO (Fig. 2D, Fig. 2E). However, this failed to reach statistical significance. When separating the cell lines within the panel into those expressing higher or lower levels of ODC1, significantly higher sensitivity to DFMO was observed in those cells expressing lower levels of ODC1 (Fig. 2F), supporting the hypothesis that in acute leukaemia cells lower ODC1 levels are associated with a higher sensitivity to DFMO.

In agreement with this finding, when narrowing down on the two leukaemia cell lines in our panel that are the most and least sensitive to DFMO, i.e. PER-485 and 697, respectively, we found them to also be on the opposite ends of the spectrum of ODC1 expression within the panel; PER-485 is the leukaemia cell line with lowest ODC1 expression, while 697 expresses some of the highest levels of ODC1 within the panel (Fig. 2D-E).

DFMO boosts polyamine uptake and polyamine transporter expression in acute leukaemia cells

We and others previously demonstrated that when polyamine biosynthesis is inhibited in solid cancer cells, cellular polyamine depletion is prevented by augmented uptake of polyamines from the surrounding environment [11-14]. We therefore investigated whether

this compensatory process also occurred in acute leukaemia cells and if so, whether this rescue effect has an impact on the leukaemia cell's sensitivity to DFMO.

We assessed the effect of DFMO treatment on polyamine uptake rates by acute leukaemia cells in polyamine uptake assays. Consistent with findings in solid cancer cell lines, treatment with DFMO significantly increased uptake of extracellular putrescine and spermidine in acute leukaemia cell lines as measured by fluorescently labelled polyamine uptake assays, in the presence and absence of aminoguanidine (Fig. 3A, Supplementary Figure 4) [24]. A comparison of the basal and DFMO-induced spermidine uptake rates in the highly DFMO-sensitive PER-485 versus the least DFMO-sensitive leukaemia cell line in the panel, 697, revealed that while baseline spermidine uptake is higher in PER-485 cells, the uptake rate of spermidine after DFMO treatment is significantly higher in 697 cells (Fig. 3B). This supports a role for polyamine uptake in mediating resistance to DFMO in acute leukaemia cells.

Sensitivity to DFMO is associated with decreased expression of polyamine transporters ATP13A2 and ATP13A3

Very little is known about the mechanisms of polyamine transport and relevant polyamine transporters in leukaemia cells. To further our understanding of the biological and functional role of polyamine transport in leukaemia cells, we investigated expression levels and prognostic relevance of transporters with well-established functions in polyamine transport and contributory roles in polyamine transport in cancer [38-46], i.e., the P5B-type ATPase family of transporters (ATP13A2-5), and the putative polyamine transporter subunit SLC3A2, for which we previously postulated a role in polyamine uptake in solid cancers [12,13].

We first assessed the expression of ATP13A2-5 and SLC3A2 in haematological cancer cell lines (BROAD cancer cell line database), and found that *SLC3A2*, *ATP13A2* and *ATP13A3* are highly expressed in leukaemia cell lines, while *ATP13A4* and *ATP13A5* are very lowly expressed (Fig. 3C). *SLC3A2*, *ATP13A2* and *ATP13A3* were thus chosen for further evaluation in our studies. High expression levels of *ATP13A2* or *SLC3A2* are associated with poor outcome in the Target B-ALL database (Fig. 3D-E). Elevated *ATP13A2* expression is also predictive of inferior survival rates in the TCGA AML patient dataset (Fig. 3D), while *ATP13A3* expression levels do not correlate with outcome (Supplementary Figure 5).

As prior studies in pancreatic cancer cells link baseline expression level of polyamine transporters to DFMO responsiveness [38,42], we next investigated variability in ATP13A2, ATP13A3 and SLC3A2 expression in relation to DFMO sensitivity. *Highly DFMO-sensitive*

leukaemia cells expressed significantly lower protein levels of ATP13A2 and ATP13A3 (Fig. 3F, Supplementary Figure 6A), and ATP13A2 and ATP13A3 protein expression were negatively correlated with DFMO sensitivity (Supplementary Fig 6B-C). Whilst SLC3A2 expression was also lower in *highly DFMO-sensitive* cells, this was not significant (Fig. 3F).

Moreover, upon evaluating the change in polyamine transporter expression when treated with DFMO, overall, levels of ATP13A3 and/or SLC3A2 were observed to increase at a certain time point in all tested leukaemia cell lines but one (Reh), while no consistent changes were observed in ATP13A2 levels (Fig. 3G). However, fold increases in DFMO-induced ATP13A3 expression were more pronounced in *less DFMO-sensitive* 697 cells versus *highly DFMO-sensitive* PER-485 cells (Fig. 3H), which corresponds to the observed higher increase in polyamine uptake in 697 cells after DFMO treatment (Fig. 3B).

Taken together, these findings suggest a potential role for polyamine transporter ATP13A2, ATP13A3 and potentially SLC3A2 in mediating DFMO-induced polyamine uptake and impacting sensitivity of the cell line to DFMO as a single agent. This observation is consistent with findings in pancreatic ductal carcinoma and neuroblastoma cells in which loss of functional ATP13A3 increases cell sensitivity to DFMO [42,46].

The polyamine transport inhibitor AMXT 1501 abrogates basal and DFMO-induced polyamine uptake and synergises with DFMO in killing leukaemia cells

The polyamine transport inhibitor AMXT 1501, in clinical trial for solid tumours in combination with DFMO (NCT05500508), has been shown to inhibit DFMO-boosted polyamine uptake in solid cancer cells and to potentiate the effects of DFMO in preclinical solid cancer models [12-14]. Upon testing AMXT 1501 in leukaemia cells, the drug abolished basal putrescine, spermidine and spermine uptake as measured in polyamine uptake experiments (Fig 4A, Supplementary Figure 7, Supplementary Figure 8). Importantly, AMXT 1501 also completely inhibited and reversed the increase in polyamine uptake induced by DFMO treatment (Fig. 4A, Supplementary Figure 7).

We subsequently assessed whether AMXT 1501 was able to potentiate the growth-inhibitory effects of DFMO on acute leukaemia cells by performing synergy viability assays combining DFMO and AMXT 1501 in a panel of acute leukaemia cell lines [47]. DFMO and AMXT 1501 synergistically inhibited the viability of all leukaemia cells tested in our panel as exemplified by positive mean Bliss sums (Fig. 4B). This enhanced inhibition was mediated by augmented induction of apoptosis (Fig. 4C). No significant correlations were observed between the level of synergy (represented by Bliss sum) and growth rate (doubling time), sensitivity to DFMO or AMXT 1501 as single agents, or expression levels of ODC1, AMD1 or the SLC3A2, ATP13A2 and ATP13A3 transporters (Supplementary

Figure 9 A-H). However, trends were noted for correlations between decreased ODC1 and ATP13A3 protein levels and enhanced synergy between DFMO and AMXT 1501 (ODC1: P=0.0735, Supplementary Figure 9D; ATP13A3: P=0.0989 Supplementary Figure 9H). When comparing the Bliss sum between different leukaemia subtypes, the two MPAL leukaemia cell lines included in the panel presented with significantly increased synergy scores (Supplementary Figure 9I). While both MPAL cell lines are characterised by the occurrence of a *KMT2A* translocation, no significant difference in synergy score was observed between *KMT2A*-wildtype and *KMT2A*-rearranged acute leukaemia cells (Supplementary Figure 9J).

c-MYC expression drives polyamine addiction in acute leukaemia cells and increases sensitivity to the combination of DFMO and AMXT 1501

Our previous work in neuroblastoma revealed that heightened polyamine pathway activity is a downstream effect of *MYCN* gene dysregulation, with the polyamine biosynthesis gene *ODC1* and the polyamine transporter gene *SLC3A2* being identified as direct transcriptional targets of *MYC* oncogenes *c-MYC* and *MYCN* [12,48]. Hyperactivated c-*MYC* has been described as a driver in leukaemia, and to investigate the association between *c-MYC* expression and sensitivity to polyamine depletion strategies in acute leukaemia, we made use of a gene expression database of a genetically engineered human lymphoblastoid cell line (P493-6) with inducible *c-MYC* silencing [49]. Upon switching off *c-MYC*, the expression of polyamine synthesis genes as well as polyamine transporter genes was significantly downregulated compared to control cells (Fig. 5A). In contrast, the expression of genes encoding enzymes involved in the breakdown of polyamines (i.e., *SAT1*, *PAOX1*, *SMOX*) was increased upon *c-MYC* silencing (Fig. 5A), suggesting that activity of the polyamine pathway and intracellular polyamine levels are regulated by this oncoprotein.

We next investigated whether similar links between *c-MYC* and polyamine pathway gene expression occurred in leukaemia patient samples using the Target II B-ALL, TCGA AML and MILE databases. Significant positive correlations between *c-MYC* expression and expression of *ODC1* were revealed in all three leukaemia databases while a correlation with polyamine transporter *ATP13A3* was found in two out of three databases (Fig. 5B). Interestingly, *c-MYC* expression did not correlate consistently with the expression of the biosynthesis gene *AMD1* or polyamine transporter gene *ATP13A2*, with a positive correlation being shown in one patient cohort and a negative correlation in another cohort (Supplementary Figure 10). No significant correlations were observed between *c-MYC* expression and *SLC3A2* expression in any of the three leukaemia databases (Supplementary Figure 10).

To evaluate whether *c-MYC* expression affects leukaemia cell responsiveness to polyamine depletion, we compared the effect of the DFMO/AMXT 1501 combination on P493-6 cell viability in the presence and absence of c-MYC (Fig. 5C, Supplementary Figure 11). In c-MYC expressing P493-6 cells, a strong synergy (high Bliss sum) was observed between DFMO and AMXT 1501 while synergy was significantly less pronounced when *c-MYC* expression was silenced (Fig. 5D-E). *c-MYC* status did not significantly interfere with P493-6 cell sensitivity to DFMO or AMXT 1501 as single agents (Supplementary Figure 12). As c-MYC expression is associated with increased expression of polyamine biosynthesis and polyamine transporter genes, suggesting that c-MYC drives both pathways of polyamine conservation for cells, c-MYC expressing cells might be particularly apt at adapting to a single event of polyamine biosynthesis inhibition or polyamine transport blockade by activating the alternative pathway. The finding that c-MYC status increases the extent of synergy between DFMO and AMXT 1501 suggests that c-MYC regulates other factors or pathways that determine responsiveness to the drug combination and extent of synergy between polyamine biosynthesis inhibition and uptake blockade, such as the activity level of polyamine catabolism. Overall, our data indicate that c-MYC contributes to hyperactivity of the polyamine pathway in leukaemia cells and drives dependency of leukaemia cells on polyamines, resulting in a higher sensitivity to polyamine depletion by DFMO and AMXT 1501.

Polyamine depletion delays leukaemia progression in xenograft models of infant *KMT2A*-rearranged ALL

To assess the therapeutic relevance of our *in vitro* findings, we next assessed the efficacy of DFMO, AMXT 1501 and their combination in mouse models of acute leukaemia that have poor survival outcomes. Infant *KMT2A*-rearranged ALL is a subtype that has one of the most inferior outcomes in children, characterised by a highly aggressive and rapidly progressing disease course, with a high unmet need for better treatment options [50]. PER-485 leukaemia cells, derived from an infant that relapsed with *KMT2A*-rearranged mixed phenotype acute leukaemia (MPAL) after an initial diagnosis of *KMT2A*-rearranged ALL, were injected intravenously into NSG mice [51]. In this systemic acute leukaemia model, leukaemia cells become detectable at low levels in the bone marrow 1.5 weeks after inoculation, followed by their dissemination into the blood, spleen and liver after which animals become moribund upon high leukaemia burden (endpoint). Treatment of the mice with DFMO, AMXT 1501, or the combination was initiated 1.5 weeks after inoculation, when bone marrow disease is present (Fig. 6A). The doses and administration schemes were chosen based on previous efficacy and tolerability studies with DFMO and AMXT 1501 and are clinically achievable in patients [12-14,52]. An additional treatment arm was included in which leukaemia-engrafted mice were treated with a combination of cytarabine and

daunorubicin, mimicking the induction chemotherapy backbone currently used for the treatment of paediatric AML. Within eleven days of treatment initiation, the percentage of human CD45$^+$ (huCD45$^+$) leukaemic blasts in the blood of vehicle-treated mice increased significantly compared to mice treated with DFMO, AMXT 1501, DFMO/AMXT 1501 or cytarabine and daunorubicin (Fig. 6B). Three days later, only mice treated with AMXT 1501 alone or DFMO/AMXT1501 had significantly lower circulating levels of leukaemic blasts compared to control mice (Fig. 6B). The combination of cytarabine and daunorubicin did not extend survival of PER-485 engrafted mice (Fig. 6C, Supplementary Table 2), demonstrating the chemotherapy-refractoriness of this leukaemia model. In contrast, both DFMO and AMXT 1501 as single agents significantly extended EFS by 20%, outperforming the chemotherapy backbone (Fig. 6C, Supplementary Table 2). Combination treatment DFMO/AMXT 1501 prolonged survival of mice by 47% compared to vehicle treatment and significantly increased EFS compared to each single agent (Fig 6C, Supplementary Table 2), demonstrating therapeutic enhancement between the two drugs *in vivo* [20].

We next evaluated the efficacy of DFMO and AMXT 1501 alone and in combination in the MLL-3 PDX model established from a patient with *KMT2A*-rearranged infant ALL with polyamine depletion treatment starting at a high level of disease burden [53]. After inoculation of *KMT2A*-rearranged ALL PDX cells by intravenous injection in NSG mice, treatment was initiated when the median percentage of huCD45$^+$ cells in the peripheral blood of the mice reached 1%, corresponding to a high disease burden (Fig. 6D). Seven days after treatment initiation, leukaemia burden in vehicle-treated mice had increased to over 30% (on average) of huCD45$^+$ leukaemic blasts in the blood (Fig. 6E). In contrast to the PER-485 model, DFMO alone did not delay leukaemia growth in this model (Fig. 6E). However, AMXT 1501 as a single agent and in combination with DFMO, significantly delayed leukaemia growth in the peripheral blood measured 1 and 2 weeks after treatment initiation (Fig. 6E). In line with these findings, DFMO as a single agent did not lead to a survival benefit, while AMXT 1501 alone significantly extended EFS by 27% compared to vehicle treatment (Fig. 6F, Supplementary Table 2). As the combination of AMXT 1501 and DFMO achieved a similar extension of survival (31%), no therapeutic enhancement was observed with the combination of the drugs in comparison to AMXT 1501 alone (Fig. 6F, Supplementary Table 2).

Taken together, our data demonstrate that polyamine depletion strategies can delay the disease progression of highly aggressive acute leukaemia subtypes, even in high disease-burden settings.

Discussion

In this study, we established that acute leukaemia cells are dependent on polyamines for their growth and survival and that dual targeting of polyamine biosynthesis and uptake delays leukaemia growth and progression in preclinical models, proposing polyamine depletion as a candidate treatment approach for further preclinical and clinical evaluation in acute leukaemias.

With the approval of clinical use of DFMO as maintenance treatment in neuroblastoma, understanding determinants of response and resistance to the drug will be important to identify those patients most likely to respond to the single agent, or those in need of supplementation with a polyamine uptake inhibitor to achieve clinical benefit. While the polyamine biosynthesis inhibitor DFMO as a single agent significantly suppressed the growth of all tested acute leukaemia cell lines, variability in response was observed. More rapidly growing cells were more responsive to DFMO, in line with previous reports linking polyamine pathway activity to tumour aggressiveness [34,36]. Diminished responsiveness to DFMO was on one hand associated with higher baseline expression of ODC1, and on the other hand with increased baseline ATP13A2, ATP13A3 and SLC3A2 polyamine transporter expression, as well as higher fold increases in polyamine uptake and polyamine transporter upregulation upon DFMO treatment. The link between high ODC1 levels and decreased sensitivity to DFMO as a single agent aligns with a previously published study in pancreatic cancer that demonstrated that high ODC1 expression was associated with diminished responsiveness of pancreatic cancer cell lines to DFMO, presumably due to the difficulty of blocking high levels of the protein with the inhibitor [38]. On the other hand, it seemingly contradicts findings in *MYCN*-amplified neuroblastoma and DIPG preclinical models that show that MYCN-expressing cells, that have high levels of ODC1, are more addicted to polyamines and thus more sensitive to polyamine biosynthesis inhibition [12,13,36,54,55].

The discerned relationship between elevated expression of polyamine transporters at baseline and after DFMO treatment, and suppressed sensitivity to DFMO, as well as the observation of higher uptake rates in the least DFMO-sensitive cell line versus the most DFMO-sensitive cell line, are both in line with polyamine uptake also constituting a resistance and rescue mechanism to DFMO in leukaemia cells. While this rescue mechanism has prior been well established in solid cancers [12,13,42,46], it has not previously been formally confirmed or validated in leukaemia cells until now. Earlier studies in the 1980s hinted at the importance of polyamine uptake from the environment by leukaemia cells in determining sensitivity and response to DFMO [56,57]. Leukaemia-engrafted mice that were fed a polyamine-deficient diet were found to be more sensitive to DFMO [57,58]. The importance of polyamine uptake was further highlighted by mouse studies where the murine lymphocytic B-cell leukaemia cell line L1210 was exposed to increasing doses of

MGBG, a spermidine analogue that is taken up by cells through the polyamine uptake system, to generate a polyamine uptake-deficient MGBG resistant cell line (L1210-MGBG^r) [59]. DFMO treatment led to a greater survival benefit in L1210-MGBG^r-engrafted mice compared to L1210-engrafted mice, indicating increased sensitivity to DFMO upon inhibition of polyamine transport [58-60]. In this study, we now provide conclusive evidence that leukaemia cells also compensate for polyamine depletion induced by inhibition of polyamine synthesis by upregulating polyamine uptake from their environment.

Our demonstration of high baseline expression levels of polyamine transporters correlating with decreased responsiveness to DFMO, disagrees with a previous report in pancreatic cancer cells [38]. Madan et al. observed that pancreatic cancer cells with higher ATP13A3 expression were more sensitive to DFMO as they were more reliant on polyamine uptake for their viability, and were similarly more responsive to combination therapy of DFMO and a polyamine transport inhibitor compared to low ATP13A3 expressing cells [38]. Nevertheless, the group demonstrated that silencing ATP13A3 in pancreatic cancer cells increased the cell's sensitivity to DFMO, which is in line with a role of the transporter in mediating resistance to DFMO [42].

While the investigations in our leukaemia cell line panel did not yield conclusive markers for DFMO/AMXT 1501 synergism, our studies in a lymphoblastoid cell line with inducible cMYC silencing suggest that cMYC hyperactivity might define a leukaemia subtype with heightened sensitivity to the dual targeting of DFMO and AMXT 1501. cMYC expression did not result in changes in the cells' sensitivity to DFMO as a single agent though, contrasting with previous findings in pancreatic cancer cells in which cMYC expression tracked with sensitivity to DFMO and increased polyamine transport [38].

The observation that increased cMyc expression in the P493-6 lymphoblastoid cell line did not change the cell line's sensitivity to DFMO, while it increased ODC1 and ATP13A3 expression, also seemingly contradicts our demonstrated links between ODC1 and polyamine transporter levels and DFMO sensitivity, and cautions for the use of singular expression levels of ODC1 and ATP13A3 in leukaemia cells to predict responsiveness to DFMO. As cMYC, similar to NMYC, impacts a myriad of metabolic pathways, and regulates the expression of a multitude of enzymes within the polyamine pathway (e.g. catabolic gene expression), the sensitivity to DFMO is likely dictated by the expression or activity of numerous pathway components, not merely by expression levels of ODC1 or ATP13A3. These results highlight the complexity of tumour metabolism and its intricate links to oncogenic drivers, as well as the difficulty to map activity of a metabolic pathway through investigating the expression level of singular pathway components. Future dedicated

biomarker studies would preferably be performed in *in vivo* models to most accurately model polyamine metabolism within an organism and include metabolomic methods to identify biomarkers of response.

Our study also highlights the need for a careful evaluation of whether transporter expression levels can be utilised as markers for polyamine uptake activity. In this work, we found on one hand that basal spermidine uptake levels were higher in *highly DFMO-sensitive* PER-485 cells than in *less DFMO-sensitive* 697 cells, while on the other hand, high baseline ATP13A2 and ATP13A3 expression levels were associated with decreased sensitivity to DFMO. This suggests that expression levels of polyamine transporters, as evaluated in immunoblotting experiments on lysates generated with buffers that also release membrane, endosomal and nuclear proteins, might not accurately represent the level of basal polyamine transport activity. This might be explained by the fact that the transporter activity of P5B-ATPases is dependent on the transporters' location. Both ATP13A2 and ATP13A3 have been shown to reside in the endo-lysosomal compartment, and ATP13A3 has also been localised in and below the surface of the plasma membrane [38,41,46,61]. Previous studies in pancreatic cancer cells indicated that DFMO treatment can induce relocalisation of ATP13A3 from the nucleolus to the plasma membrane in some pancreatic cancer cells [38], suggesting that its activity is dependent on its location, information which is lacking from Western blotting on bulk cell lysates and would require detailed localisation studies. It is possible that total cellular transporter levels are more representative for polyamine transport capacity upon stress or polyamine depletion conditions, with those cells expressing high levels of transporters being able to adapt more quickly to these stress conditions by their ability to more rapidly redistribute transporters and activate enhanced polyamine uptake. Another explanation of our findings exists in the possibility that other transporters than ATP13A2 and ATP13A3 are important for polyamine uptake in acute leukaemia cells.

While transporters of the P5B-ATPase family have previously been linked to different cancer types [39], and SLC3A2 has been proposed as a polyamine transporter subunit in neuroblastoma and DIPG [12,13], this is the first report on a putative role for ATP13A2 and ATP13A3 in acute leukaemia. Our observation that sensitivity to DFMO correlated with decreased baseline levels of the polyamine transporters ATP13A2 and ATP13A3, suggest a key role of these transporters to polyamine uptake in acute leukaemia cells. Moreover, the association between heightened expression of polyamine transporters ATP13A2 and SLC3A2 and inferior outcome in patients with acute leukaemia, provides further evidence for a contribution of polyamine uptake to leukaemia progression.

In conclusion, this study provides evidence that polyamine depletion by dual targeting of polyamine biosynthesis and polyamine uptake inhibits acute leukaemia cell survival and progression of aggressive and treatment-resistant leukaemia. Our findings support further preclinical and clinical investigations to determine the therapeutic potential of this strategy for acute leukaemia.

Ethics statement

All animal experiments were approved by the University of New South Wales Animal Care and Ethics Committee according to the Animal Research Act 1985, and the Australian Code of Practice for Care and Use of Animals for Scientific Purposes.

Acknowledgements

Children's Cancer Institute Australia is affiliated with UNSW Sydney and the Sydney Children's Hospitals Network.

Conflicts of Interest

M.B. is the Founder, President and CSO at Aminex Therapeutics where he is an employee and stock owner. P.V. participates in polyamine transporter drug screening efforts for cancer and Parkinson's disease.

Author Contributions

The work reported in the paper has been performed by the authors, unless clearly specified in the text. K.S. and L.X. conceptualized the study with contributions of M.D.N and M.H. All experiments were performed by W.G., M.K., with support by A.K., D.S., E.R. and A.B.. W.G. and K.S. analysed the data. K.S. led the project. L.C.C., R.S.K. and R.B.L. provided access to leukaemia models and expertise in leukaemia animal models. S.H.L.V. provided the BODIPY-labelled polyamines. K. T. kindly shared Polyamine-RED. X.G. and C.M. performed survival and gene expression (RNAseq) analyses. M.R. B. provided AMXT 1501 for this study. M.A. and P.V. contributed expertise in polyamine transporters. K.S. wrote the first draft of the manuscript, which has been edited by W.G., M.K., M.D.N and M.H. All authors have read and approved the manuscript.

Data Availability Statement

The data that support the findings of this study are available from the corresponding author upon reasonable request.

Disclaimer

The authors have no disclaimers to report.

Funding

This work was supported by a grant from Cancer Australia and the Kids' Cancer Project (PdCCRS, APP1188234) given to M.D.N., M.H., L.X. and K.S., by the FWO research grants (G094219N and G009324N) and the C1 KU Leuven research grant InterAction (C14/21/095) to P.V.. R.B.L. and M.H. are supported by Fellowships from the Australian National Health and Medical Research Council (1157871, 2017256 respectively).

References

1. Kantarjian H, Kadia T, DiNardo C, et al. Acute myeloid leukemia: current progress and future directions. Blood Cancer J 2021;11(2):41. DOI: 10.1038/s41408-021-00425-3.
2. Reedijk AMJ, Klein K, Coebergh JWW, et al. Improved survival for children and young adolescents with acute myeloid leukemia: a Dutch study on incidence, survival and mortality. Leukemia 2019;33(6):1349-1359. DOI: 10.1038/s41375-018-0314-7.
3. Pegg AE. Polyamine metabolism and its importance in neoplastic growth and a target for chemotherapy. Cancer Res 1988;48(4):759-74. (https://www.ncbi.nlm.nih.gov/pubmed/3123052).
4. Casero RA, Jr., Murray Stewart T, Pegg AE. Polyamine metabolism and cancer: treatments, challenges and opportunities. Nat Rev Cancer 2018;18(11):681-695. DOI: 10.1038/s41568-018-0050-3.
5. Oesterheld J, Ferguson W, Kraveka JM, et al. Eflornithine as Postimmunotherapy Maintenance in High-Risk Neuroblastoma: Externally Controlled, Propensity Score-Matched Survival Outcome Comparisons. J Clin Oncol 2024;42(1):90-102. DOI: 10.1200/JCO.22.02875.
6. Sholler GLS, Ferguson W, Bergendahl G, et al. Maintenance DFMO Increases Survival in High Risk Neuroblastoma. Sci Rep 2018;8(1):14445. DOI: 10.1038/s41598-018-32659-w.
7. Millward MJ, Joshua A, Kefford R, et al. Multi-centre Phase II trial of the polyamine synthesis inhibitor SAM486A (CGP48664) in patients with metastatic melanoma. Invest New Drugs 2005;23(3):253-6. DOI: 10.1007/s10637-005-6734-z.
8. Simoneau AR, Gerner EW, Nagle R, et al. The effect of difluoromethylornithine on decreasing prostate size and polyamines in men: results of a year-long phase IIb randomized placebo-controlled chemoprevention trial. Cancer Epidemiol Biomarkers Prev 2008;17(2):292-9. DOI: 10.1158/1055-9965.EPI-07-0658.
9. Siimes M, Seppanen P, Alhonen-Hongisto L, Janne J. Synergistic action of two polyamine antimetabolites leads to a rapid therapeutic response in childhood leukemia. Int J Cancer 1981;28(5):567-70. DOI: 10.1002/ijc.2910280506.
10. Gastaut JA, Tell G, Schechter PJ, Maraninchi D, Mascret B, Carcassonne Y. Treatment of acute myeloid leukemia and blastic phase of chronic myeloid leukemia with combined eflornithine (alpha difluoromethylornithine) and methylglyoxal-bis-guanyl hydrazone (methyl-GAG). Cancer Chemother Pharmacol 1987;20(4):344-8. DOI: 10.1007/BF00262590.

11. Aziz SM, Gillespie MN, Crooks PA, et al. The potential of a novel polyamine transport inhibitor in cancer chemotherapy. J Pharmacol Exp Ther 1996;278(1):185-92. (https://www.ncbi.nlm.nih.gov/pubmed/8764350).
12. Gamble LD, Purgato S, Murray J, et al. Inhibition of polyamine synthesis and uptake reduces tumor progression and prolongs survival in mouse models of neuroblastoma. Sci Transl Med 2019;11(477). DOI: 10.1126/scitranslmed.aau1099.
13. Khan A, Gamble LD, Upton DH, et al. Dual targeting of polyamine synthesis and uptake in diffuse intrinsic pontine gliomas. Nat Commun 2021;12(1):971. DOI: 10.1038/s41467-021-20896-z.
14. Samal K, Zhao P, Kendzicky A, et al. AMXT-1501, a novel polyamine transport inhibitor, synergizes with DFMO in inhibiting neuroblastoma cell proliferation by targeting both ornithine decarboxylase and polyamine transport. Int J Cancer 2013;133(6):1323-33. DOI: 10.1002/ijc.28139.
15. Pirnes-Karhu S, Jantunen E, Mäntymaa P, Mustjoki S, Alhonen L, Uimari A. Spermidine/spermine N(1)-acetyltransferase activity associates with white blood cell count in myeloid leukemias. Exp Hematol 2014;42(7):574-80. (In eng). DOI: 10.1016/j.exphem.2014.02.008.
16. Tripathi AK, Chaturvedi R, Ahmad R, et al. Peripheral blood leucocytes ornithine decarboxylase activity in chronic myeloid leukemia patients: prognostic and therapeutic implications. Leuk Res 2002;26(4):349-54. (In eng). DOI: 10.1016/s0145-2126(01)00142-4.
17. Sari IN, Yang YG, Wijaya YT, et al. AMD1 is required for the maintenance of leukemic stem cells and promotes chronic myeloid leukemic growth. Oncogene 2021;40(3):603-617. DOI: 10.1038/s41388-020-01547-x.
18. Shardakov VI, Dem'ianova VT, Kopaneva TG. [Immunosuppressive action of polyamines in patients with chronic myeloid leukemia]. Gematol Transfuziol 1994;39(1):9-11. (https://www.ncbi.nlm.nih.gov/pubmed/8188035).
19. Somers K, Chudakova DA, Middlemiss SM, et al. CCI-007, a novel small molecule with cytotoxic activity against infant leukemia with MLL rearrangements. Oncotarget 2016;7(29):46067-46087. DOI: 10.18632/oncotarget.10022.
20. Somers K, Evans K, Cheung L, et al. Effective targeting of NAMPT in patient-derived xenograft models of high-risk pediatric acute lymphoblastic leukemia. Leukemia 2020;34(6):1524-1539. DOI: 10.1038/s41375-019-0683-6.
21. Di Veroli GY, Fornari C, Wang D, et al. Combenefit: an interactive platform for the analysis and visualization of drug combinations. Bioinformatics 2016;32(18):2866-8. DOI: 10.1093/bioinformatics/btw230.
22. Karsa M, Kosciolek A, Bongers A, et al. Exploiting the reactive oxygen species imbalance in high-risk paediatric acute lymphoblastic leukaemia through auranofin. Br J Cancer 2021;125(1):55-64. DOI: 10.1038/s41416-021-01332-x.
23. Somers K, Kosciolek A, Bongers A, et al. Potent antileukemic activity of curaxin CBL0137 against MLL-rearranged leukemia. Int J Cancer 2020;146(7):1902-1916. DOI: 10.1002/ijc.32582.
24. Houdou M, Jacobs N, Coene J, et al. Novel Green Fluorescent Polyamines to Analyze ATP13A2 and ATP13A3 Activity in the Mammalian Polyamine Transport System. Biomolecules 2023;13(2) (In eng). DOI: 10.3390/biom13020337.
25. Somers K, Wen VW, Middlemiss SMC, et al. A novel small molecule that kills a subset of MLL-rearranged leukemia cells by inducing mitochondrial dysfunction. Oncogene 2019;38(20):3824-3842. DOI: 10.1038/s41388-018-0666-5.

26. Bots M, Verbrugge I, Martin BP, et al. Differentiation therapy for the treatment of t(8;21) acute myeloid leukemia using histone deacetylase inhibitors. Blood 2014;123(9):1341-52. DOI: 10.1182/blood-2013-03-488114.
27. Baker A, Gregory GP, Verbrugge I, et al. The CDK9 Inhibitor Dinaciclib Exerts Potent Apoptotic and Antitumor Effects in Preclinical Models of MLL-Rearranged Acute Myeloid Leukemia. Cancer Res 2016;76(5):1158-69. DOI: 10.1158/0008-5472.CAN-15-1070.
28. Khan A, Gamble LD, Upton DH, et al. Dual targeting of polyamine synthesis and uptake in diffuse intrinsic pontine gliomas. Nature Communications 2021;12(1):971. DOI: 10.1038/s41467-021-20896-z.
29. Rose WC, Wild R. Therapeutic synergy of oral taxane BMS-275183 and cetuximab versus human tumor xenografts. Clin Cancer Res 2004;10(21):7413-7. DOI: 10.1158/1078-0432.CCR-04-1045.
30. Kees UR, Ford J, Watson M, et al. Gene expression profiles in a panel of childhood leukemia cell lines mirror critical features of the disease. Mol Cancer Ther 2003;2(7):671-7. (https://www.ncbi.nlm.nih.gov/pubmed/12883040).
31. Sharmin S, Sakata K, Kashiwagi K, et al. Polyamine Cytotoxicity in the Presence of Bovine Serum Amine Oxidase. Biochemical and Biophysical Research Communications 2001;282(1):228-235. DOI: https://doi.org/10.1006/bbrc.2001.4569.
32. Wang L, Liu Y, Qi C, et al. Oxidative degradation of polyamines by serum supplement causes cytotoxicity on cultured cells. Scientific Reports 2018;8(1):10384. DOI: 10.1038/s41598-018-28648-8.
33. Moshier JA, Dosescu J, Skunca M, Luk GD. Transformation of NIH/3T3 cells by ornithine decarboxylase overexpression. Cancer Res 1993;53(11):2618-22. (In eng).
34. Auvinen M, Paasinen A, Andersson LC, Holtta E. Ornithine decarboxylase activity is critical for cell transformation. Nature 1992;360(6402):355-8. DOI: 10.1038/360355a0.
35. Paasinen-Sohns A, Kielosto M, Kaariainen E, et al. c-Jun activation-dependent tumorigenic transformation induced paradoxically by overexpression or block of S-adenosylmethionine decarboxylase. J Cell Biol 2000;151(4):801-10. DOI: 10.1083/jcb.151.4.801.
36. Geerts D, Koster J, Albert D, et al. The polyamine metabolism genes ornithine decarboxylase and antizyme 2 predict aggressive behavior in neuroblastomas with and without MYCN amplification. Int J Cancer 2010;126(9):2012-24. DOI: 10.1002/ijc.25074.
37. Lozier AM, Rich ME, Grawe AP, et al. Targeting ornithine decarboxylase reverses the LIN28/Let-7 axis and inhibits glycolytic metabolism in neuroblastoma. Oncotarget 2015;6(1):196-206. DOI: 10.18632/oncotarget.2768.
38. Madan M, Patel A, Skruber K, Geerts D, Altomare DA, Phanstiel O. ATP13A3 and caveolin-1 as potential biomarkers for difluoromethylornithine-based therapies in pancreatic cancers. Am J Cancer Res 2016;6(6):1231-52. (In eng).
39. Azfar M, van Veen S, Houdou M, Hamouda NN, Eggermont J, Vangheluwe P. P5B-ATPases in the mammalian polyamine transport system and their role in disease. Biochim Biophys Acta Mol Cell Res 2022;1869(12):119354. (In eng). DOI: 10.1016/j.bbamcr.2022.119354.
40. van Veen S, Martin S, Van den Haute C, et al. ATP13A2 deficiency disrupts lysosomal polyamine export. Nature 2020;578(7795):419-424. DOI: 10.1038/s41586-020-1968-7.

41. Hamouda NN, Van den Haute C, Vanhoutte R, et al. ATP13A3 is a major component of the enigmatic mammalian polyamine transport system. J Biol Chem 2021;296:100182. DOI: 10.1074/jbc.RA120.013908.
42. Sekhar V, Andl T, Phanstiel O. ATP13A3 facilitates polyamine transport in human pancreatic cancer cells. Scientific Reports 2022;12(1):4045. DOI: 10.1038/s41598-022-07712-4.
43. Zheng K, Li T. Prediction of ATPase cation transporting 13A2 molecule in Petromyzon marinus and pan-cancer analysis into human tumors from an evolutionary perspective. Immunogenetics 2021;73(4):277-289. (In eng). DOI: 10.1007/s00251-021-01216-7.
44. Bierkens M, Krijgsman O, Wilting SM, et al. Focal aberrations indicate EYA2 and hsa-miR-375 as oncogene and tumor suppressor in cervical carcinogenesis. Genes Chromosomes Cancer 2013;52(1):56-68. (In eng). DOI: 10.1002/gcc.22006.
45. Lek SM, Li K, Tan QX, et al. Pairing a prognostic target with potential therapeutic strategy for head and neck cancer. Oral Oncol 2020;111:105035. (In eng). DOI: 10.1016/j.oraloncology.2020.105035.
46. Azfar M, Gao W, Van den Haute C, et al. The polyamine transporter ATP13A3 mediates DFMO-induced polyamine uptake in neuroblastoma. bioRxiv 2024:2024.02.20.581161. DOI: 10.1101/2024.02.20.581161. *Accepted for publication in Molecular Oncology Nov 2024.*
47. Bliss CI. The calculation of microbial assays. Bacteriol Rev 1956;20(4):243-58. DOI: 10.1128/br.20.4.243-258.1956.
48. Bachmann AS, Geerts D. Polyamine synthesis as a target of MYC oncogenes. J Biol Chem 2018;293(48):18757-18769. DOI: 10.1074/jbc.TM118.003336.
49. Schuhmacher M, Staege MS, Pajic A, et al. Control of cell growth by c-Myc in the absence of cell division. Curr Biol 1999;9(21):1255-8. DOI: 10.1016/s0960-9822(99)80507-7.
50. Kotecha RS. Updates in infant acute lymphoblastic leukemia and the potential for targeted therapy. Hematology Am Soc Hematol Educ Program 2022;2022(1):611-617. (In eng). DOI: 10.1182/hematology.2022000359.
51. Cheung LC, de Kraa R, Oommen J, et al. Preclinical Evaluation of Carfilzomib for Infant KMT2A-Rearranged Acute Lymphoblastic Leukemia. Front Oncol 2021;11:631594. (In eng). DOI: 10.3389/fonc.2021.631594.
52. Hayes CS, Shicora AC, Keough MP, Snook AE, Burns MR, Gilmour SK. Polyamine-blocking therapy reverses immunosuppression in the tumor microenvironment. Cancer immunology research 2014;2(3):274-285.
53. Richmond J, Carol H, Evans K, et al. Effective targeting of the P53-MDM2 axis in preclinical models of infant MLL-rearranged acute lymphoblastic leukemia. Clin Cancer Res 2015;21(6):1395-405. (In eng). DOI: 10.1158/1078-0432.Ccr-14-2300.
54. Hogarty MD, Norris MD, Davis K, et al. ODC1 is a critical determinant of MYCN oncogenesis and a therapeutic target in neuroblastoma. Cancer Res 2008;68(23):9735-45. (In eng). DOI: 10.1158/0008-5472.Can-07-6866.
55. Auvinen M, Jarvinen K, Hotti A, et al. Transcriptional regulation of the ornithine decarboxylase gene by c-Myc/Max/Mad network and retinoblastoma protein interacting with c-Myc. Int J Biochem Cell Biol 2003;35(4):496-521. DOI: 10.1016/s1357-2725(02)00305-9.
56. Dorhout B, Ferwerda H, Kingma AW, de Hoog E, Muskiet FA. In vivo manipulation of L1210 cell cycle phase distribution with alpha-difluoromethylornithine, 4-

amidinoindan-1-one 2'-amidinohydrazone and N1-acetylspermine. Biochim Biophys Acta 1998;1381(1):89-94. DOI: 10.1016/s0304-4165(98)00015-4.
57. Nakaike S, Kashiwagi K, Terao K, Iio K, Igarashi K. Combined use of alpha-difluoromethylornithine and an inhibitor of S-adenosylmethionine decarboxylase in mice bearing P388 leukemia or Lewis lung carcinoma. Jpn J Cancer Res 1988;79(4):501-8. (In eng). DOI: 10.1111/j.1349-7006.1988.tb01619.x.
58. Ask A, Persson L, Heby O. Increased survival of L1210 leukemic mice by prevention of the utilization of extracellular polyamines. Studies using a polyamine-uptake mutant, antibiotics and a polyamine-deficient diet. Cancer Lett 1992;66(1):29-34. (In eng). DOI: 10.1016/0304-3835(92)90276-2.
59. Mandel JL, Flintoff WF. Isolation of mutant mammalian cells altered in polyamine transport. J Cell Physiol 1978;97(3 Pt 1):335-43. DOI: 10.1002/jcp.1040970308.
60. Persson L, Holm I, Ask A, Heby O. Curative effect of DL-2-difluoromethylornithine on mice bearing mutant L1210 leukemia cells deficient in polyamine uptake. Cancer Res 1988;48(17):4807-11. (https://www.ncbi.nlm.nih.gov/pubmed/3136913).
61. Liu B, Azfar M, Legchenko E, et al. ATP13A3 variants promote pulmonary arterial hypertension by disrupting polyamine transport. Cardiovasc Res 2024;120(7):756-768. DOI: 10.1093/cvr/cvae068.

Figure legends

Figure 1: Heightened activity of the polyamine biosynthesis pathway is predictive of inferior outcome in acute leukaemia and the polyamine biosynthesis inhibitor DFMO inhibits growth of acute leukaemia cells by inducing apoptosis

(A) Schematic of polyamine biosynthesis enzymes. Ornithine decarboxylase 1 (ODC1) is the rate-limiting enzyme in the polyamine biosynthesis pathway that catalyses conversion of ornithine into putrescine. Adenosylmethionine decarboxylase 1 (AMD1) produces an intermediate needed for spermidine and spermine synthesis. Spermidine synthase (SRM) and spermine synthase (SMS) catalyse the production of spermidine and spermine, respectively. (B) Polyamine biosynthesis scores were calculated for bone marrow mononuclear cell samples in the MILE database (Healthy controls: N=73; B-ALL: N=576; T-ALL: N=174; AML: N=542), as a weighted average of expression decile as determined from RNA sequencing data of *ODC1*, *AMD1*, *SRM* and *SMS*. Stars above violin plots correspond to P-values for the comparison of mean biosynthesis scores of leukaemia groups versus healthy controls as determined by one-way ANOVA with Dunn's multiple comparison. (C-D) Survival analysis of leukaemia patients in the Target II paediatric B-ALL cohort (N=105) and the TCGA AML cohort (N=161) with patients segregated into high and low *ODC1* expressing groups based on upper-quartile expression level as a cut-off. (E) Cells were treated with 0.5 mM or 5 mM DFMO with or without pretreatment with an equimolar (1 μM or 10 μM) mix of exogenous polyamines (PA: putrescine, spermidine, spermine) in the presence of 1 mM aminoguanidine, an amine oxidase inhibitor that

suppresses the degradation of exogenous polyamines into toxic byproducts in culture medium containing foetal bovine serum. Viable cell number was determined by trypan blue exclusion assay. The significance of the difference in viable cell number between treatment conditions at day 3 and day 6 were determined by one-way ANOVA. The stars corresponding to significance levels for the 3 day data are presented in front of "/", while the significance of the 6 day data are presented as stars behind "/". Data represented correspond to mean $\pm$ SEM of three independent experiments. (F) Bars represent the mean increase in percentage of Annexin V^+ cells relative to untreated cells, as determined in 3 independent experiments, with or without exogenous polyamine addition, in the presence of 1 mM aminoguanidine. P-values for comparisons to untreated cells (0%) were determined by one-sample T-test and P-values for comparisons between treatments were calculated by one-way ANOVA. Stars above bars represent the significance of the comparisons to untreated cells. (G) Immunoblotting on lysates from cells treated with 2 mM DFMO or left untreated (No Tx) for 72 hours. Representative blots for 2 independent experiments per cell line are shown. *, $P<0.05$; **, $p<0.01$; ***, $P<0.001$; ****, $P<0.0001$; ns, not significant.

Figure 2: DFMO inhibits growth in a molecularly diverse panel of acute leukaemia cell lines

(A) Cells were treated with DFMO or left untreated for up to 6 days and live cells were counted by trypan blue exclusion. The significance of the difference in viable cell number between DFMO-treated and untreated cells at day 3 and day 6 was determined by Student's t-test. (B) Immunoblotting on cells treated with 2 mM DFMO or left untreated (No Tx) for 72 hours. Immunoblotting was performed once for both cell lines. (C) *Highly DFMO-sensitive* cells have a significantly shorter doubling time than the *less DFMO-sensitive* cells. P-values were calculated by Student T-test. (D) *ODC1* mRNA levels were normalised to *GUSB* mRNA expression to accommodate for variability in RNA input, and to mean relative expression across the panel. Each dot represents the mean relative mRNA expression of a cell line within the panel, derived from two independent experiments. Correlation analysis (Pearson) was performed between *ODC1* relative expression and sensitivity to DFMO (represented by % DFMO-induced growth inhibition). (E) Immunoblot for ODC1 in a panel of acute leukaemia cell lines, representative of two independent experiments. Ponceau staining of whole protein lysate was performed to control for differences in total protein levels loaded and for normalisation purposes. To combine densitometric quantification data obtained from two separate blots, data were normalised to that of cell lysates that were included on both blots. Each dot represents the mean relative protein expression of a cell line derived from two independent experiments. (F) Cell lines were separated into those expressing higher or lower levels of ODC1, with the

cut-off defined as the mean of the relative ODC1 protein expression across the panel. The difference of DFMO sensitivity between high and low ODC1 protein groups is tested with Student T-test. *, P<0.05; **, p<0.01; ***, P<0.001; ****, P<0.0001; ns, not significant.

Figure 3: DFMO treatment boosts polyamine uptake and polyamine transporter expression in acute leukaemia cells

(A) After 24 hours of DFMO treatment (1mM), BODIPY (BDP)-labelled polyamines were added for 30 min in the presence of aminoguanidine (1 mM), after which the uptake rate of BODIPY(BDP)-labelled polyamines was measured. Bars represent the mean geo MFI (% relative to untreated control cells) of at least two independent experiments. The significance of the change in uptake relative to untreated cells (100%) was determined by one-sample T-test. (B) After 72 hours of DFMO (2 mM) treatment, BODIPY (BDP)-labelled spermidine (BDP-SPD) was added for 30 min in the presence of aminoguanidine (1 mM), followed by a measurement of BDP-SPD uptake rate. Bars represent the mean Geo MFI of three independent experiments. Mean Geo MFI between groups were compared by One-way ANOVA. (C) Polyamine transporter expression in the MILE database. (D) Patients from the Target II paediatric B-ALL and TCGA AML cohorts were separated into those having high versus low *ATP13A2* expression based on the upper quartile expression level as cut-off. (E) Patients from the Target II paediatric B-ALL cohort were segregated based on the upper quartile expression of *SLC3A2* as a cut-off. (F) Polyamine transporter levels were compared between *highly DFMO-sensitive* and *less DFMO-sensitive* leukaemia cells. Each dot represents the mean relative transporter protein expression of a cell line as determined in two independently executed immunoblotting experiments (normalised to actin and to the mean expression level across the panel). Means between groups were compared by Student's t-test. (G) Polyamine transporter levels in leukaemia cells upon DFMO treatment. Immunoblotting representative of two independent experiments. The displayed ACTIN panel for the Reh and CEM cells is the same as shown for those cells in Figure 2G as immunoblotting for CASPASE-3 was performed on the same blot. (H) Quantification of ATP13A3 protein bands in western blotting of lysates of untreated and DFMO-treated (2 mM, 72h) PER-485 and 697 cells. Full-length ATP13A3 densitometry measurements were normalised to Ponceau S densitometry measurements. Bars represent the full-length ATP13A3 protein levels of two independent experiments. Expression levels were compared by One-way ANOVA. *, P<0.05; **, p<0.01; ***, P<0.001; ****, P<0.0001; ns, not significant.

Figure 4: AMXT 1501 abrogates DFMO-induced polyamine uptake and synergises with DFMO in killing acute leukaemia cells

(A-B) Cells were treated with DFMO (1mM, 24 hours), after which BODIPY (BDP)-labelled polyamines were added for 30 min in the presence of aminoguanidine (1 mM) followed by the measurement of BDP-labelled polyamine uptake. Bars represent the mean he mean percentage Geo MFI (% of untreated control cells) of at least two independent experiments. Asterisks on the bars represent P-values calculated by one sample t-test determining whether there is a statistically significant change in the mean % Geo MFI of treated cells versus untreated cells (100%). Stars above lines correspond to P-values calculated by one-way ANOVA. (B) 6x6 matrix synergy assay representative for at least two independently executed synergy assays, measuring resazurin-reduction based viability after 72h exposure. (C) Bars represent the mean increase in percentage of Annexin V^+ cells relative to untreated cells, as determined in 3 independent experiments. P-values for comparisons to untreated cells (0%) were determined by one-sample T-test (asterisks above bars) and P-values for comparisons between treatments were calculated by one-way ANOVA (stars above lines). Asterisks represent the significance of the comparisons to untreated cells. *, $p<0.05$; **, $p<0.01$; ***, $P<0.001$; ****, $P<0.0001$.

Figure 5: Induced *c-MYC* expression increases sensitivity to polyamine depletion (A) mRNA expression of polyamine synthesis genes (top row), polyamine transporter genes (middle row) and polyamine catabolism genes (bottom row) in P493-6 cells with or without (presence of tetracycline) *c-MYC* expression. Gene expression data were obtained from the Gene Expression Omnibus site (Accession no. 107222). The relative gene expression of each biological replicate (n=4) is represented by a colour scale, with red indicating high expression level, green representing low expression level. (B) Correlation analyses (Pearson) for *c-MYC* mRNA and *ODC1* or *ATP13A3* mRNA expression levels in patients with leukaemia from three databases. (C) Schematic of the experimental workflow of matrix synergy assays performed with P493-6 cells. On day 0, doxycycline (1 µg/mL) was added to P493-6 cells for 72h to silence c-MYC expression. Cells were seeded and treated with increasing concentrations of DFMO and AMXT 1501 in a 6x6 matrix format in the presence of doxycycline (1 µg/mL). Cell viability is determined 72h later using resazurin reduction-based assays. Drug interaction effects were analyzed by Combenefit and evaluated according to the Bliss Independence model. (D) Evaluation of synergy between DFMO and AMXT 1501 by 6x6 matrix synergy assays. Represented synergy data are representative of at least two independently executed synergy assays, measuring resazurin reduction-based viability after a 72h exposure. (E) Bars represent mean Bliss scores $\pm$ SE of three independent experiments. Student T-test was used to evaluate the difference between the Bliss scores of c-MYC on and off cells. *, $p<0.05$.

Figure 6: Polyamine depletion slows progression of *KMT2A*-rearranged infant leukaemia models

(A) Design of the *in vivo* study for the PER-485 xenograft model. DFMO (1%) was added into drinking water until endpoint was reached and AMXT 1501 (1.25 mg/kg) was subcutaneously injected daily for 17 days. For the combination arm, DFMO and AMXT 1501 were administered according to their individual regimens. Chemotherapy was administered via intraperitoneal injection: 25 mg/kg (four days on/three days off) for cytarabine and 0.625 mg/kg (one day on/ six days off) for daunorubicin (1 injection) for two cycles. (B) Percentage human $CD45^+$ cells ($HuCD45^+$), relative to the total of mouse $CD45^+$ ($mCD45^+$) and $huCD45^+$ cells, in the peripheral blood of PER-485 engrafted mice. (C) Kaplan-Meier survival curves were compared by Gehan-Wilcoxon. (D) Design of the *in vivo* study for the MLL-3 PDX model. (E) Percentage $huCD45^+$ cells (relative to $mCD45^+$ and $huCD45^+$ cells) in the peripheral blood of MLL-3 engrafted mice. F) Kaplan-Meier survival curves were compared by Gehan-Wilcoxon. Mice were treated as described for A. *, $p<0.05$; **, $p<0.01$**; $P<0.001$; ****, $P<0.0001$.

Figure 1

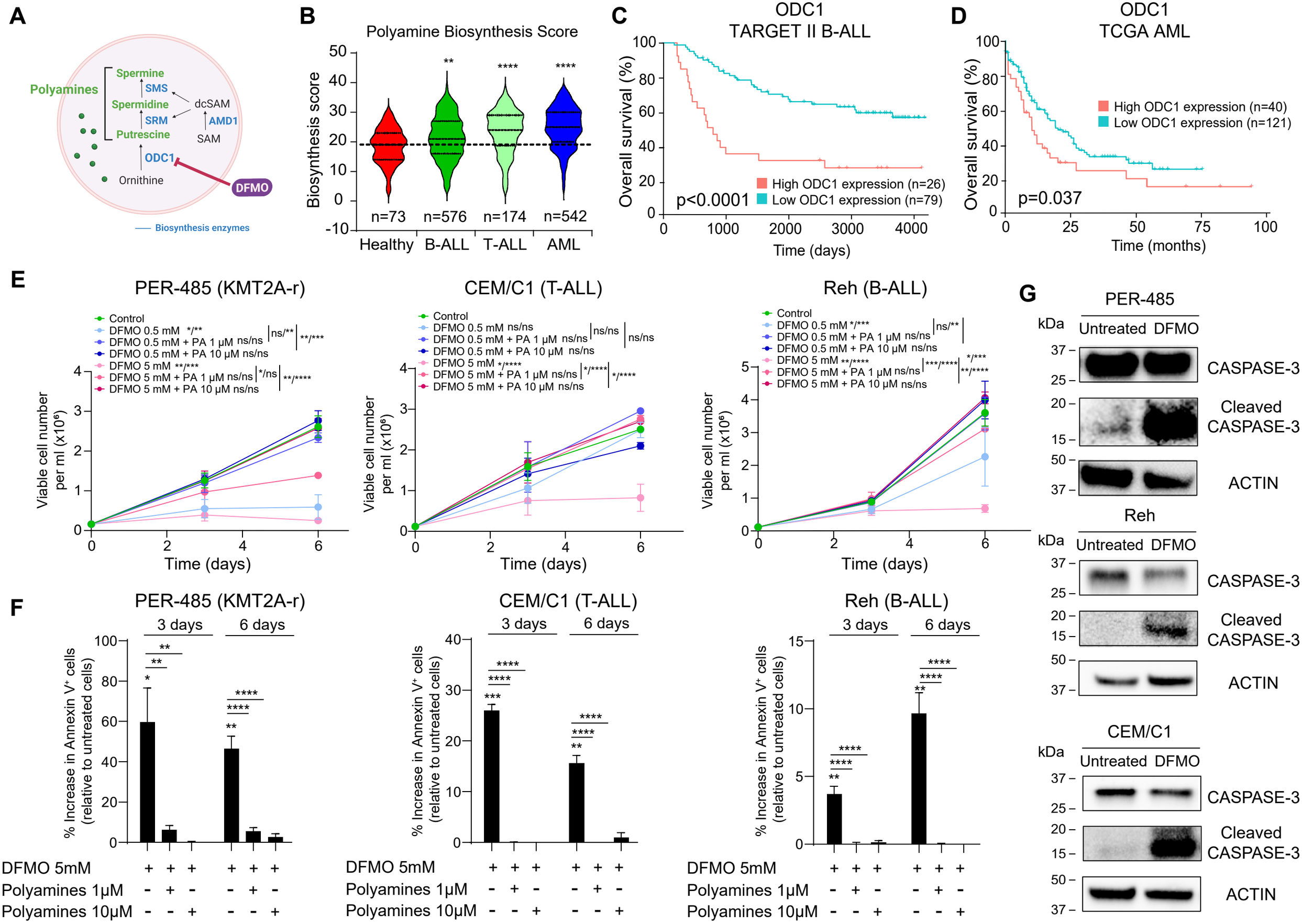
A
Polyamines
Spermine
SMS
Spermidine
SRM
Putrescine
dcSAM
AMD1
SAM
ODC1
Ornithine
DFMO
Biosynthesis enzymes
B
Polyamine Biosynthesis Score
Biosynthesis score
n=73
n=576
n=174
n=542
Healthy
B-ALL
T-ALL
AML
C
ODC1
TARGET II B-ALL
Overall survival (%)
p<0.0001
High ODC1 expression (n=26)
Low ODC1 expression (n=79)
Time (days)
D
ODC1
TCGA AML
Overall survival (%)
p=0.037
High ODC1 expression (n=40)
Low ODC1 expression (n=121)
Time (months)
E
PER-485 (KMT2A-r)
CEM/C1 (T-ALL)
Reh (B-ALL)
Control
DFMO 0.5 mM
DFMO 0.5 mM + PA 1 µM
DFMO 0.5 mM + PA 10 µM
DFMO 5 mM
DFMO 5 mM + PA 1 µM
DFMO 5 mM + PA 10 µM
Viable cell number per ml (x10⁶)
Time (days)
F
PER-485 (KMT2A-r)
CEM/C1 (T-ALL)
Reh (B-ALL)
3 days
6 days
% Increase in Annexin V⁺ cells (relative to untreated cells)
DFMO 5mM
Polyamines 1µM
Polyamines 10µM
G
PER-485
Reh
CEM/C1
kDa
Untreated
DFMO
CASPASE-3
Cleaved CASPASE-3
ACTIN

Figure 2

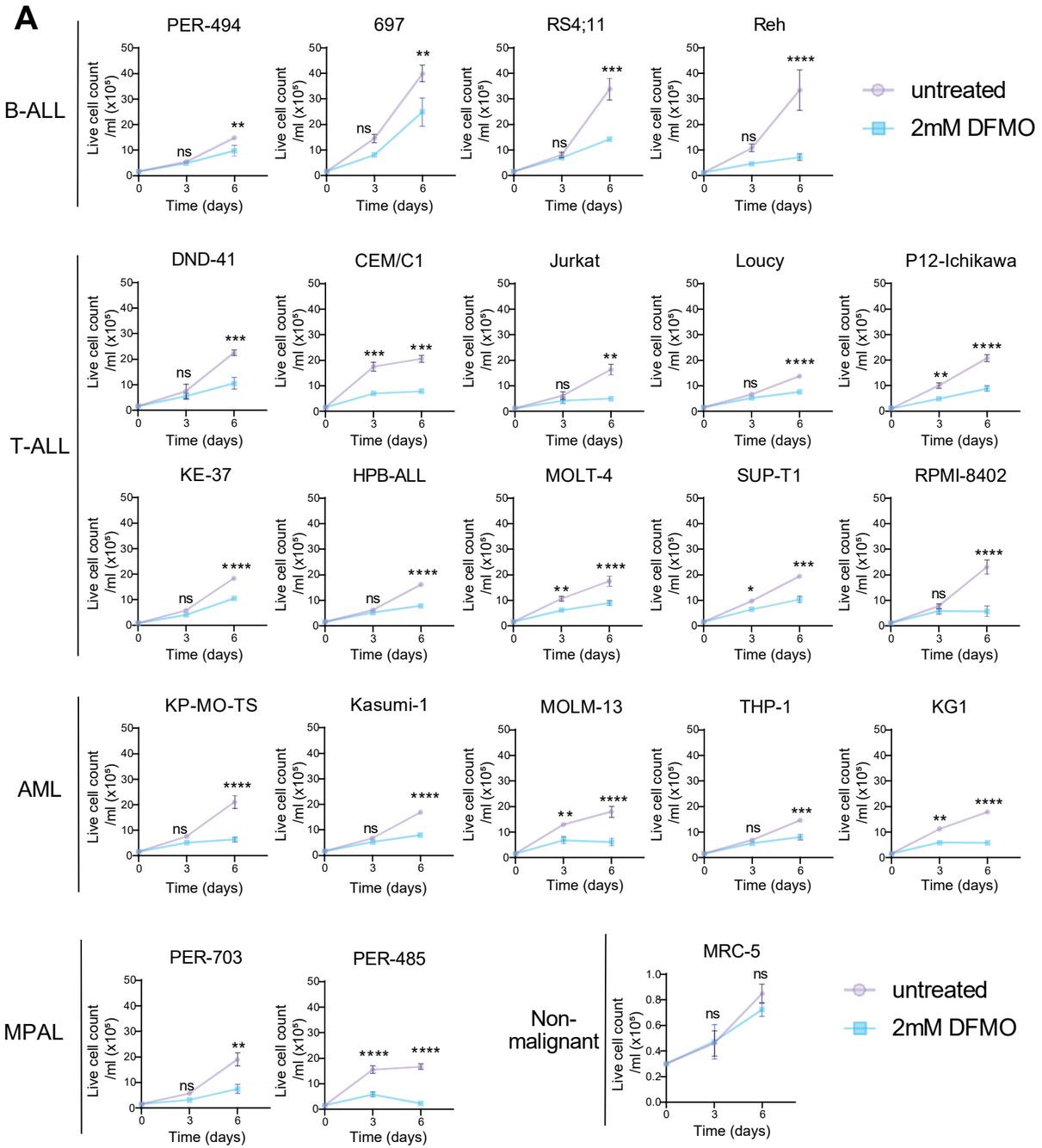
A
B-ALL
T-ALL
AML
MPAL
Non-malignant
PER-494
697
RS4;11
Reh
DND-41
CEM/C1
Jurkat
Loucy
P12-Ichikawa
KE-37
HPB-ALL
MOLT-4
SUP-T1
RPMI-8402
KP-MO-TS
Kasumi-1
MOLM-13
THP-1
KG1
PER-703
PER-485
MRC-5
Live cell count /ml (x10⁵)
Time (days)
ns
*
**
***
****
untreated
2mM DFMO

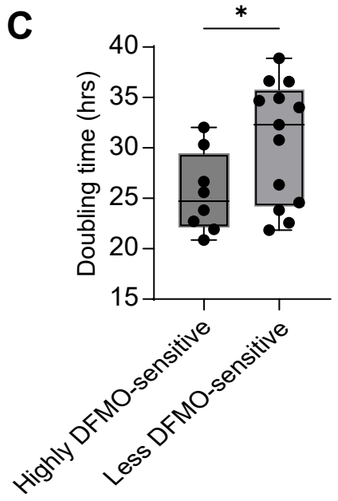
C
Doubling time (hrs)
Highly DFMO-sensitive
Less DFMO-sensitive
*

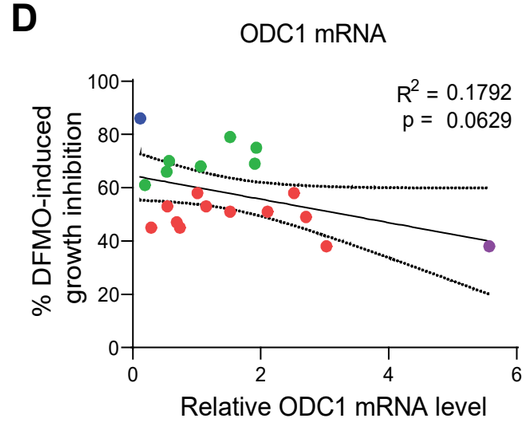
D
ODC1 mRNA
R² = 0.1792
p = 0.0629
% DFMO-induced growth inhibition
Relative ODC1 mRNA level
PER-485
697
Highly DFMO-sensitive cells
Less DFMO-sensitive cells

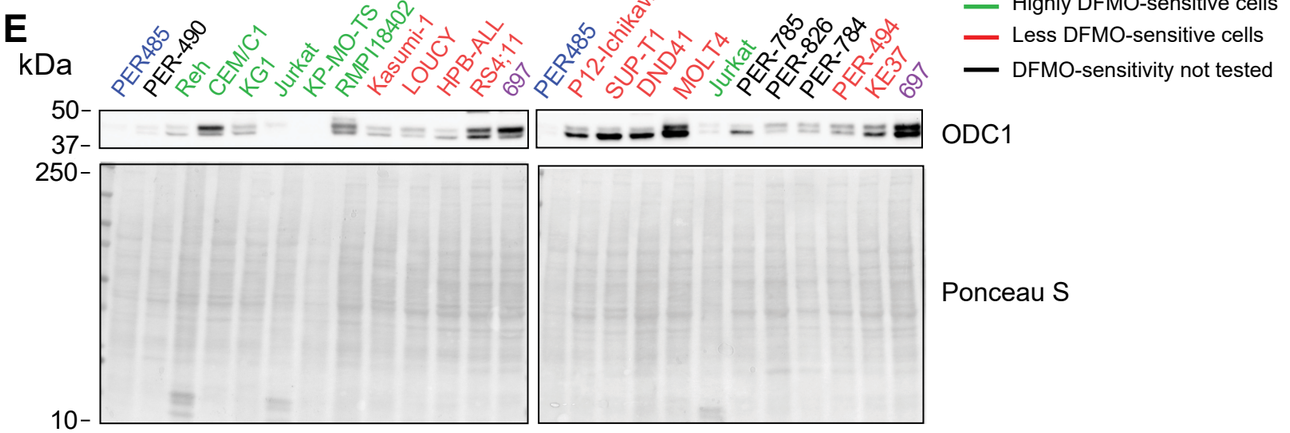
E
kDa
PER485
PER-490
Reh
CEM/C1
KG1
Jurkat
KP-MO-TS
RMPI8402
Kasumi-1
LOUCY
HPB-ALL
RS4;11
697
PER485
P12-Ichikawa
SUP-T1
DND41
MOLT4
Jurkat
PER-785
PER-826
PER-784
PER-494
KE37
697
50-
37-
ODC1
250-
10-
Ponceau S
Highly DFMO-sensitive cells
Less DFMO-sensitive cells
DFMO-sensitivity not tested

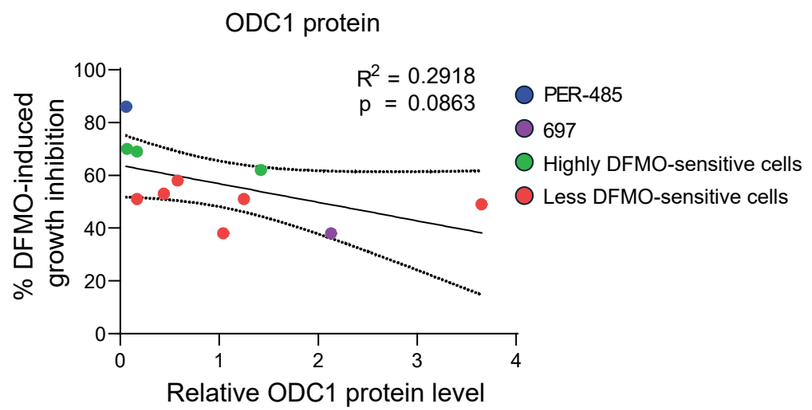
ODC1 protein
R² = 0.2918
p = 0.0863
% DFMO-induced growth inhibition
Relative ODC1 protein level
PER-485
697
Highly DFMO-sensitive cells
Less DFMO-sensitive cells

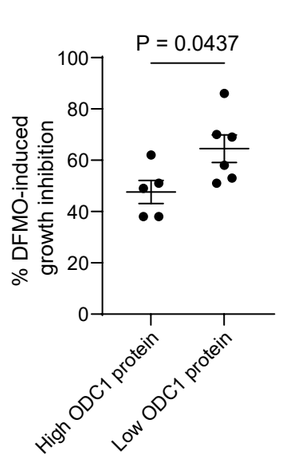
F
P = 0.0437
% DFMO-induced growth inhibition
High ODC1 protein
Low ODC1 protein

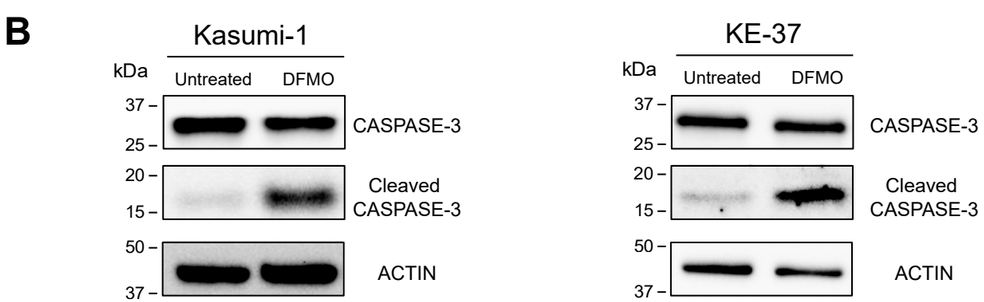
B
Kasumi-1
KE-37
kDa
Untreated
DFMO
37-
25-
20-
15-
50-
CASPASE-3
Cleaved CASPASE-3
ACTIN

Figure 3

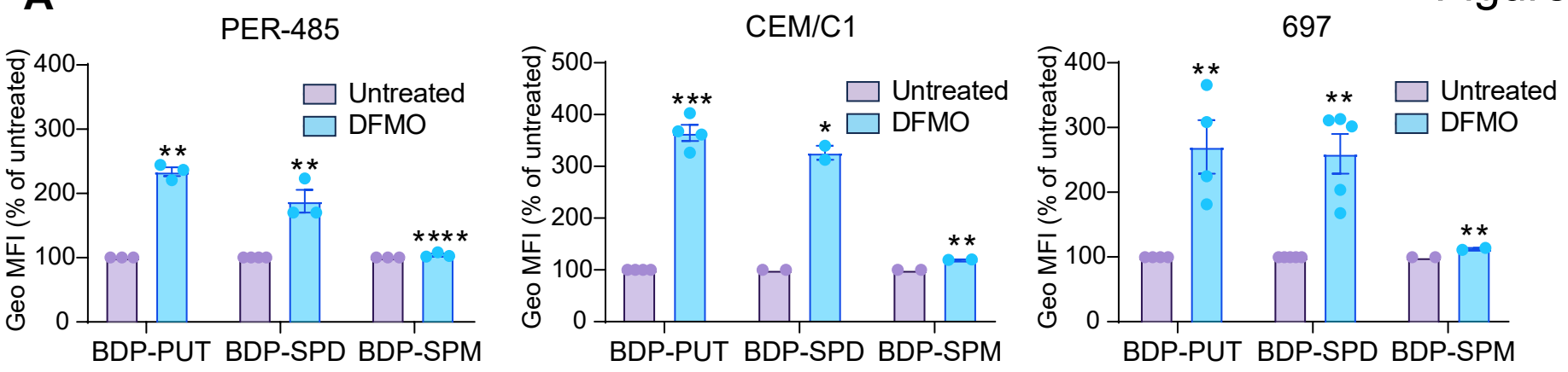
A
PER-485
CEM/C1
697
Geo MFI (% of untreated)
Untreated
DFMO
BDP-PUT
BDP-SPD
BDP-SPM

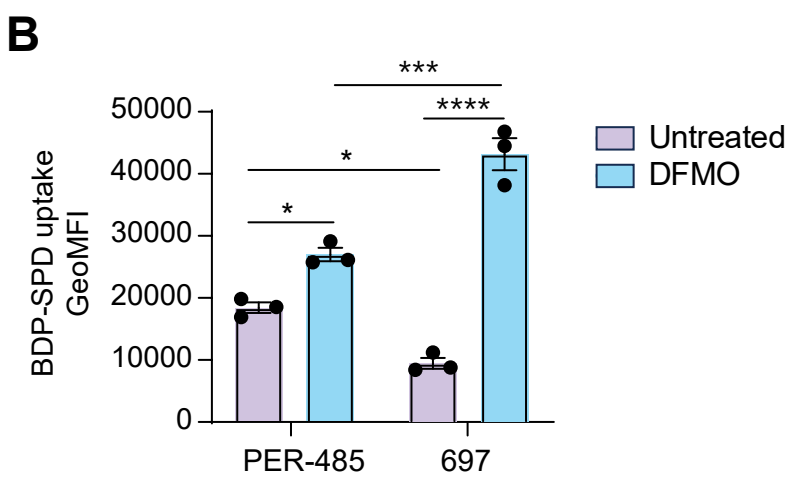
B
BDP-SPD uptake GeoMFI
Untreated
DFMO
PER-485
697

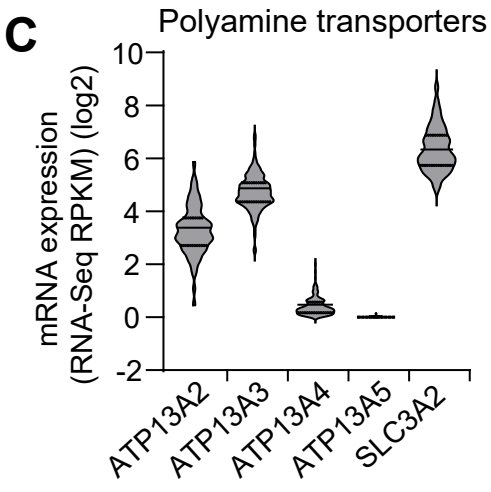
C
Polyamine transporters
mRNA expression (RNA-Seq RPKM) (log2)
ATP13A2
ATP13A3
ATP13A4
ATP13A5
SLC3A2

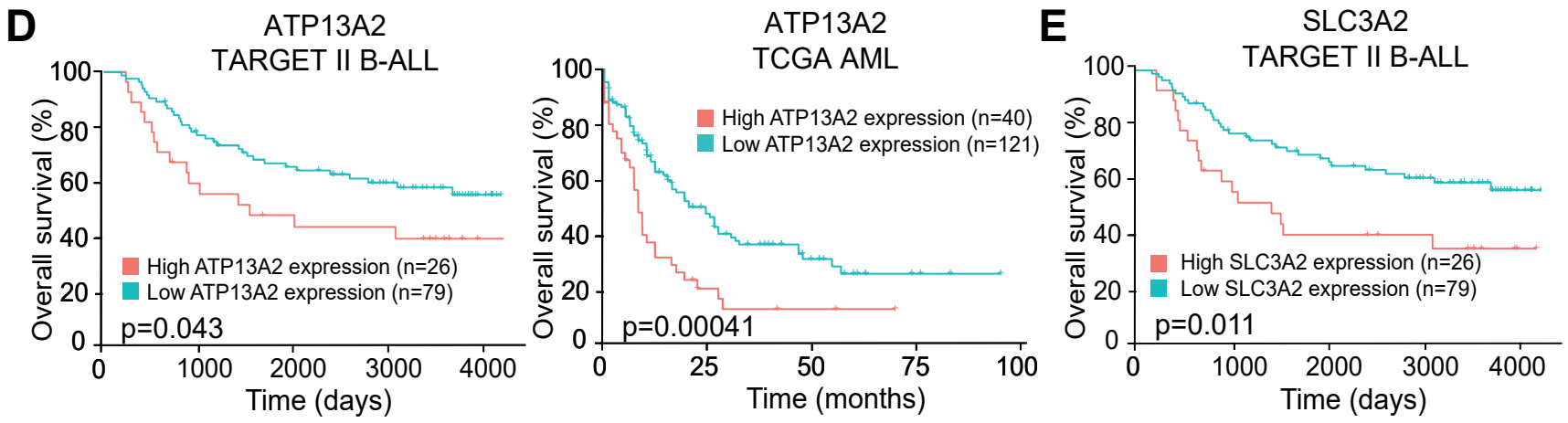
D
ATP13A2
TARGET II B-ALL
Overall survival (%)
High ATP13A2 expression (n=26)
Low ATP13A2 expression (n=79)
p=0.043
Time (days)
ATP13A2
TCGA AML
High ATP13A2 expression (n=40)
Low ATP13A2 expression (n=121)
p=0.00041
Time (months)
E
SLC3A2
TARGET II B-ALL
High SLC3A2 expression (n=26)
Low SLC3A2 expression (n=79)
p=0.011
Time (days)

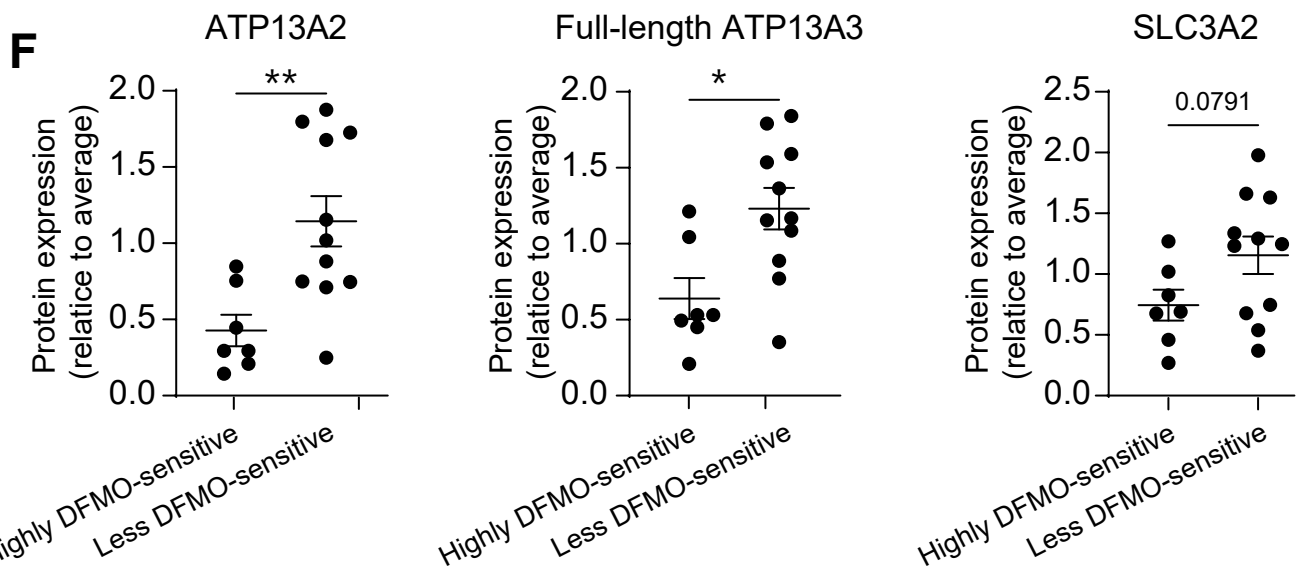
F
ATP13A2
Full-length ATP13A3
SLC3A2
Protein expression (relatice to average)
0.0791
Highly DFMO-sensitive
Less DFMO-sensitive

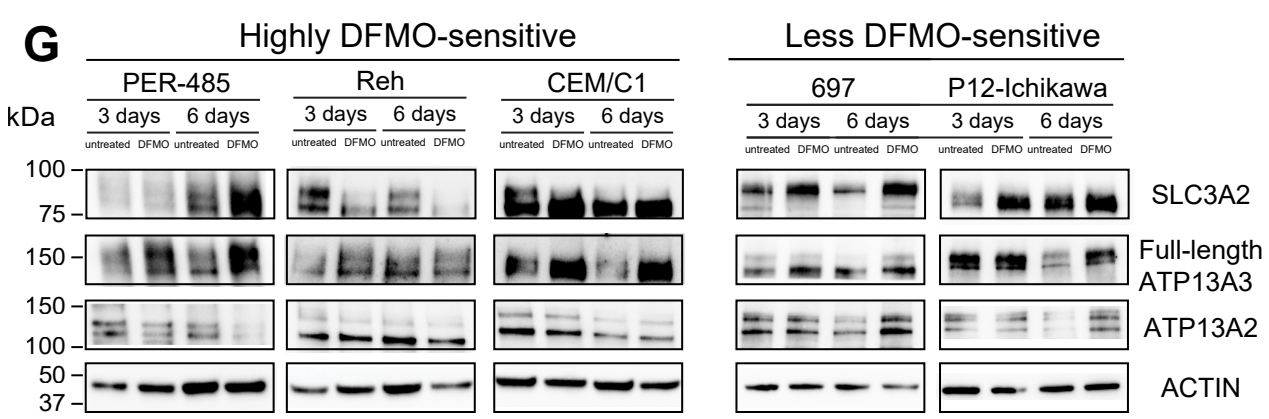
G
Highly DFMO-sensitive
Less DFMO-sensitive
PER-485
Reh
CEM/C1
697
P12-Ichikawa
kDa
3 days
6 days
untreated
DFMO
SLC3A2
Full-length ATP13A3
ATP13A2
ACTIN

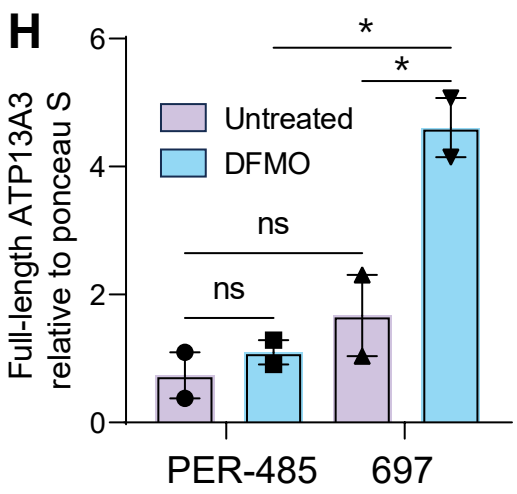
H
Full-length ATP13A3 relative to ponceau S
Untreated
DFMO
ns
PER-485
697

Figure 4

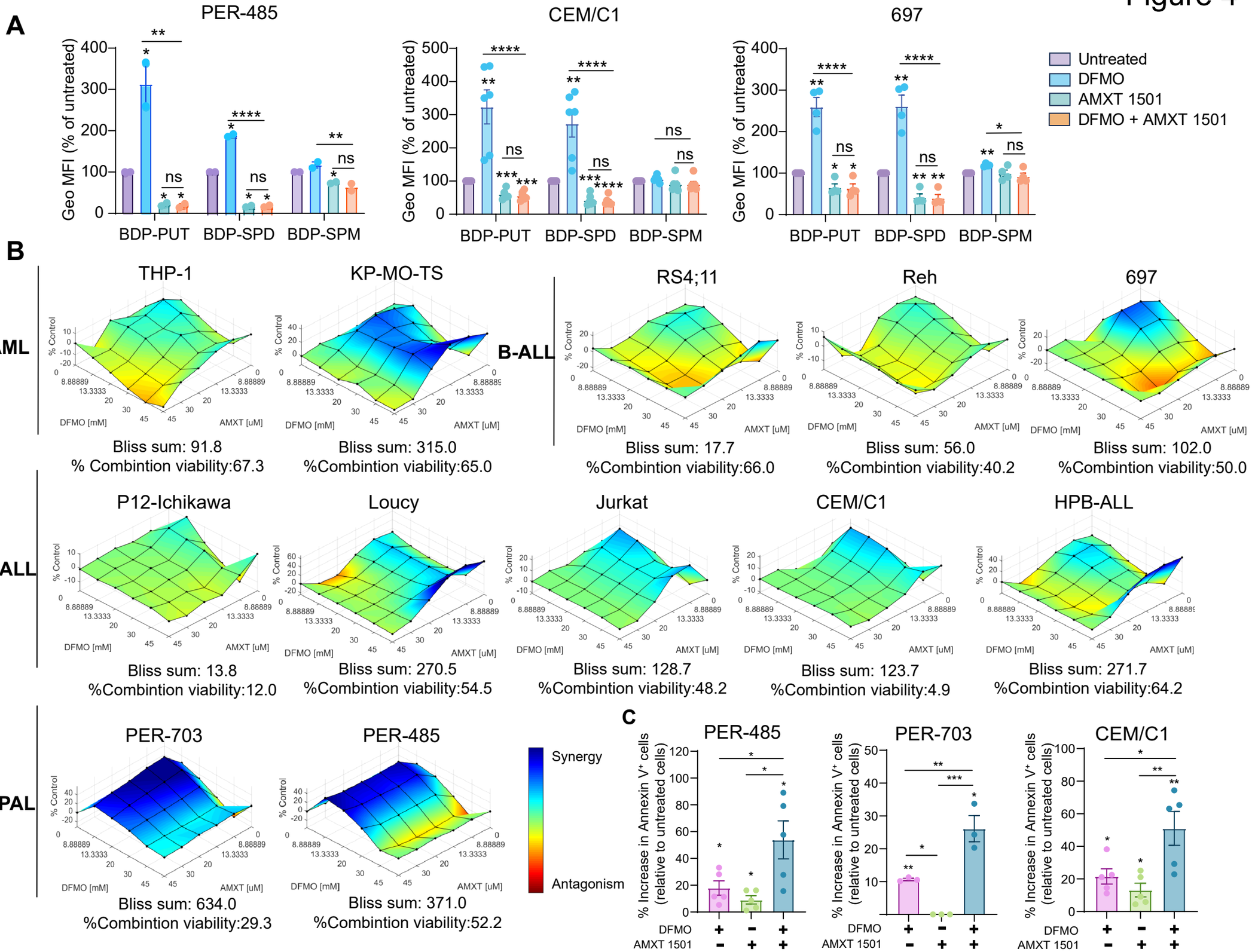
A
PER-485
CEM/C1
697
Geo MFI (% of untreated)
BDP-PUT
BDP-SPD
BDP-SPM
Untreated
DFMO
AMXT 1501
DFMO + AMXT 1501
B
AML
B-ALL
T-ALL
MPAL
THP-1
KP-MO-TS
RS4;11
Reh
697
P12-Ichikawa
Loucy
Jurkat
CEM/C1
HPB-ALL
PER-703
PER-485
% Control
DFMO [mM]
AMXT [uM]
Bliss sum: 91.8
% Combintion viability:67.3
Bliss sum: 315.0
%Combintion viability:65.0
Bliss sum: 17.7
%Combintion viability:66.0
Bliss sum: 56.0
%Combintion viability:40.2
Bliss sum: 102.0
%Combintion viability:50.0
Bliss sum: 13.8
%Combintion viability:12.0
Bliss sum: 270.5
%Combintion viability:54.5
Bliss sum: 128.7
%Combintion viability:48.2
Bliss sum: 123.7
%Combintion viability:4.9
Bliss sum: 271.7
%Combintion viability:64.2
Bliss sum: 634.0
%Combintion viability:29.3
Bliss sum: 371.0
%Combintion viability:52.2
Synergy
Antagonism
C
PER-485
PER-703
CEM/C1
% Increase in Annexin V+ cells
(relative to untreated cells)
DFMO
AMXT 1501

Figure 5

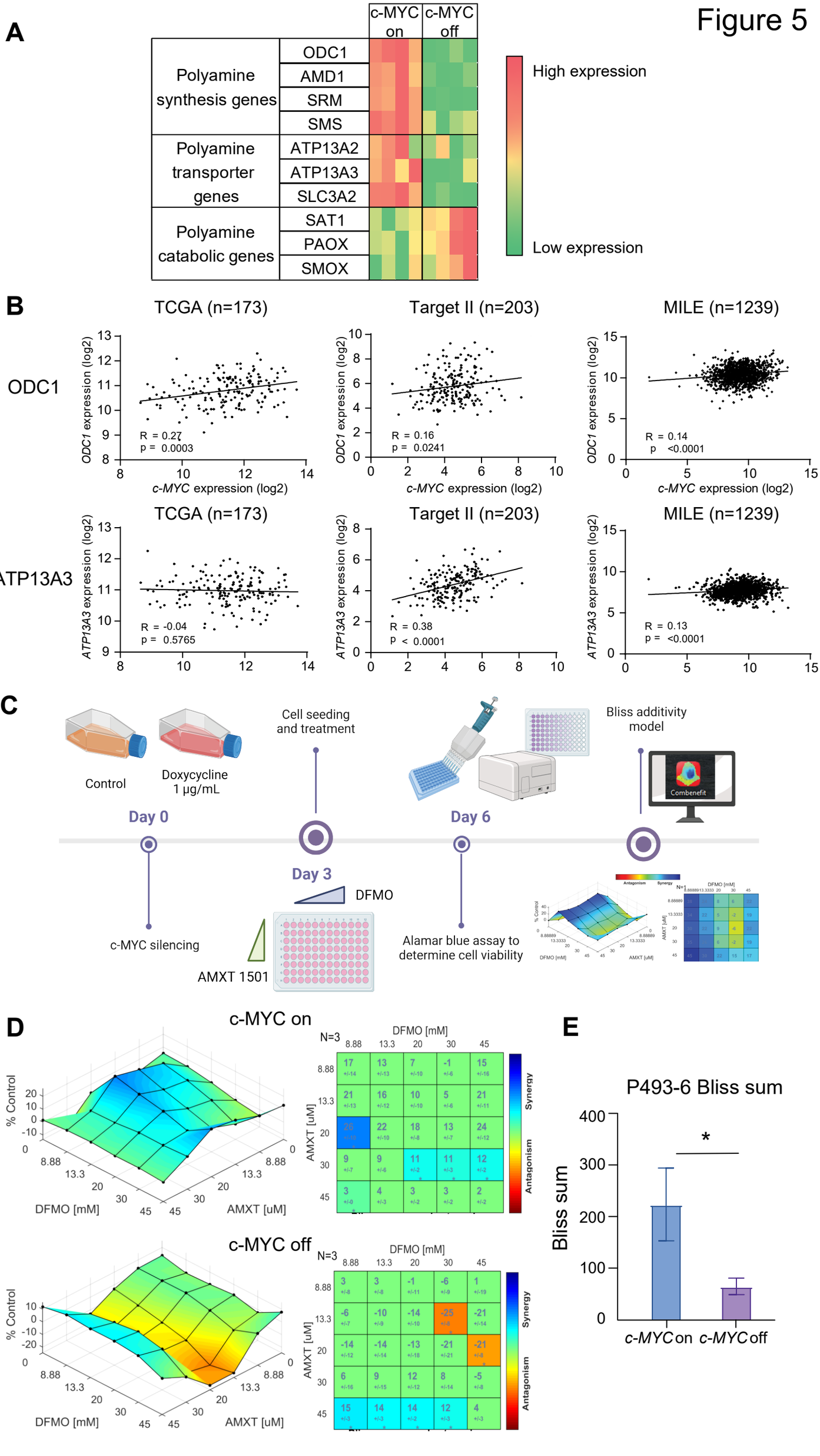
A
c-MYC on
c-MYC off
Polyamine synthesis genes
ODC1
AMD1
SRM
SMS
Polyamine transporter genes
ATP13A2
ATP13A3
SLC3A2
Polyamine catabolic genes
SAT1
PAOX
SMOX
High expression
Low expression
B
TCGA (n=173)
Target II (n=203)
MILE (n=1239)
ODC1
ODC1 expression (log2)
c-MYC expression (log2)
R = 0.27
p = 0.0003
R = 0.16
p = 0.0241
R = 0.14
p <0.0001
ATP13A3
ATP13A3 expression (log2)
R = -0.04
p = 0.5765
R = 0.38
p < 0.0001
R = 0.13
p = <0.0001
C
Control
Doxycycline 1 µg/mL
Cell seeding and treatment
Bliss additivity model
Combenefit
Day 0
Day 3
Day 6
DFMO
AMXT 1501
c-MYC silencing
Alamar blue assay to determine cell viability
D
c-MYC on
c-MYC off
% Control
DFMO [mM]
AMXT [uM]
N=3
Synergy
Antagonism
E
P493-6 Bliss sum
Bliss sum
*
c-MYCon
c-MYCoff

Figure 6

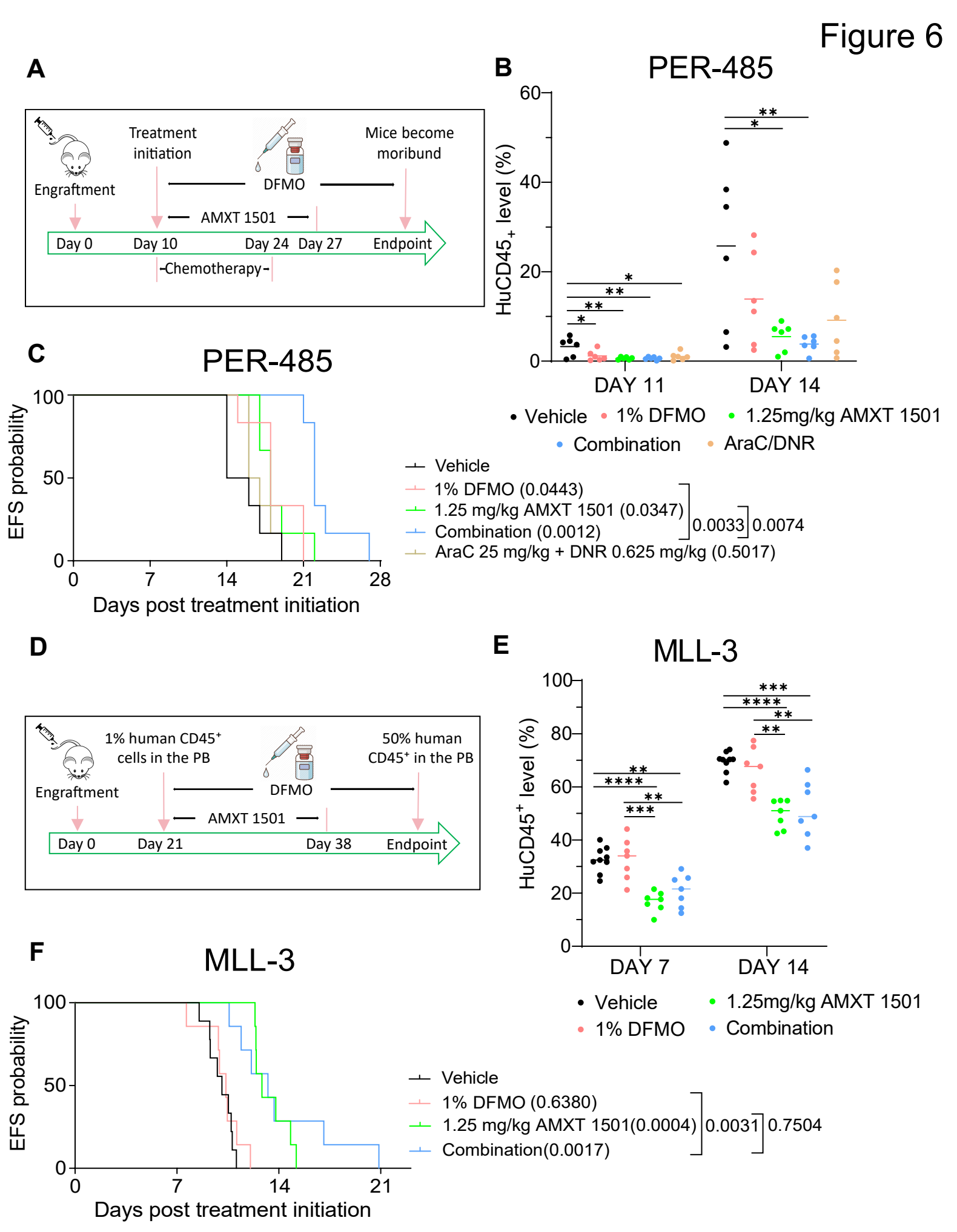
A
Engraftment
Treatment initiation
DFMO
Mice become moribund
AMXT 1501
Day 0
Day 10
Day 24
Day 27
Endpoint
-Chemotherapy-
B
PER-485
HuCD45+ level (%)
DAY 11
DAY 14
Vehicle
1% DFMO
1.25mg/kg AMXT 1501
Combination
AraC/DNR
C
PER-485
EFS probability
Days post treatment initiation
Vehicle
1% DFMO (0.0443)
1.25 mg/kg AMXT 1501 (0.0347)
Combination (0.0012)
AraC 25 mg/kg + DNR 0.625 mg/kg (0.5017)
0.0033
0.0074
D
Engraftment
1% human CD45+ cells in the PB
DFMO
50% human CD45+ in the PB
AMXT 1501
Day 0
Day 21
Day 38
Endpoint
E
MLL-3
HuCD45+ level (%)
DAY 7
DAY 14
Vehicle
1% DFMO
1.25mg/kg AMXT 1501
Combination
F
MLL-3
EFS probability
Days post treatment initiation
Vehicle
1% DFMO (0.6380)
1.25 mg/kg AMXT 1501(0.0004)
Combination(0.0017)
0.0031
0.7504

Supplementary Figures

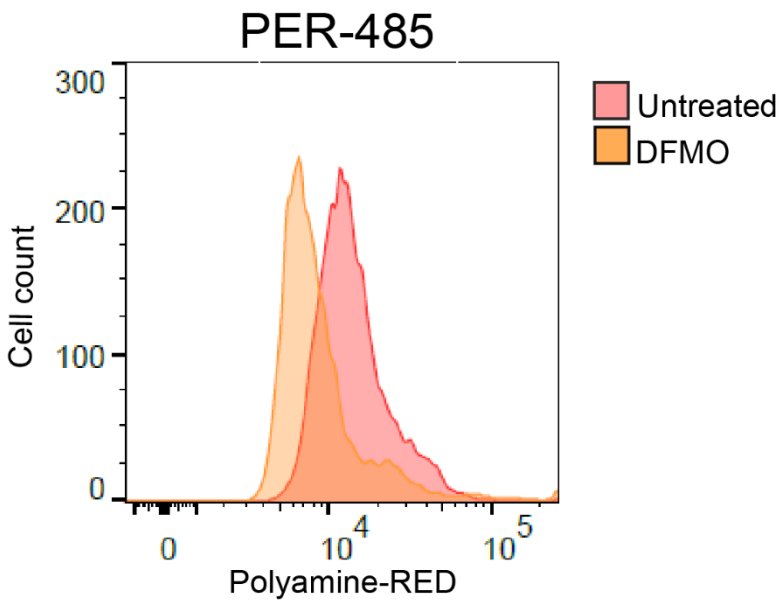

Supplementary Figure 1: DFMO decreases intracellular polyamine levels in leukaemia cells. PER-485 cells were treated with DFMO (0.5 mM) for 72 hours after which cells were stained with Polyamine-RED, a dye that stains polyamines, and fluorescence was measured by flow cytometry. Representative result from two independent biological replicates.

A

DFMO sensitivity group	Cell line	% growth inhibition	Disease
Highly DFMO-sensitive	PER-485	86	MPAL
	Reh	79	B-ALL
	RPMI-8402	75	T-ALL
	KP-MO-TS	70	AML
	Jurkat	69	T-ALL
	KG1	68	AML
	MOLM-13	66	AML
	CEM/C1	62	T-ALL
	PER-703	61	B-ALL
Less DFMO-sensitive	RS4;11	58	B-ALL
	P12-Ichikawa	58	T-ALL
	DND-41	53	T-ALL
	Kasumi-1	53	AML
	HPB-ALL	51	T-ALL
	KE-37	51	T-ALL
	MOLT-4	49	T-ALL
	SUP-T1	47	T-ALL
	THP-1	45	AML
	Loucy	45	T-ALL
	PER-494	38	B-ALL
	697	38	B-ALL

B

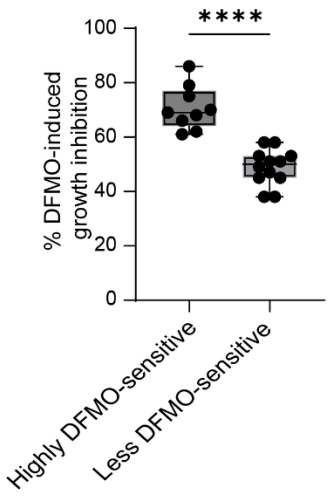

Supplementary Figure 2: Acute leukaemia cells display variable responsiveness to DFMO. A) Growth inhibition is calculated based on the percentage of live cells after a 6-day DFMO treatment, relative to the number of untreated live cells on day 6. Leukaemia cells were divided into *highly DFMO-sensitive* (% growth inhibition >60%) or *less DFMO-sensitive* cells (% growth inhibition ≤ 60%) based on the magnitude of the DFMO-induced growth inhibition. B) The mean growth inhibition induced by DFMO in *highly DFMO-sensitive* cells is significantly greater than that achieved in the *less DFMO-sensitive* cells. Means were compared by Student t-test. ****, P<0.0001.

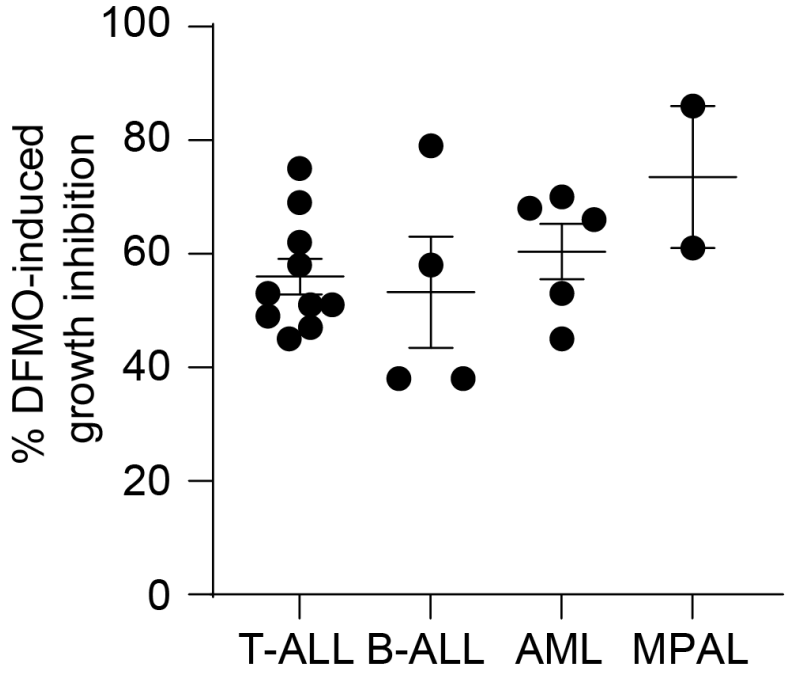

Supplementary Figure 3: No association between sensitivity to DFMO and acute leukaemia immunophenotype. There were no significant differences in % growth inhibition induced by DFMO between T-ALL, B-ALL, AML or MPAL leukaemia cell lines in our leukaemia cell line panel.

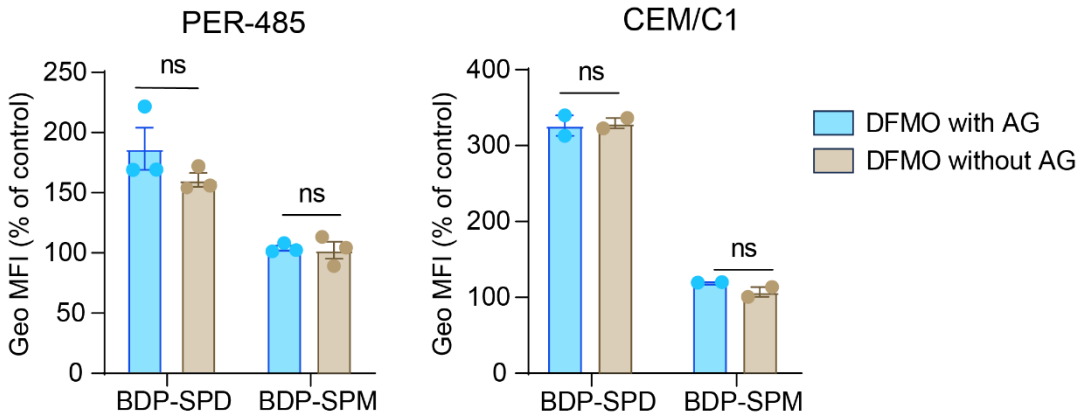

Supplementary Figure 4: Presence of aminoguanidine does not impact DFMO-induced changes in spermidine or spermine uptake in acute leukaemia cells. After 24 hours of DFMO treatment (1mM), the uptake rate of BODIPY(BDP)-labelled polyamines was measured in the presence or absence of aminoguanidine (1 mM, AG). Bars represent the mean geo MFI (% relative to untreated control cells) of at least two independent experiments. Mean Geo MFI between groups were compared by Student T-test. ns, not significant.

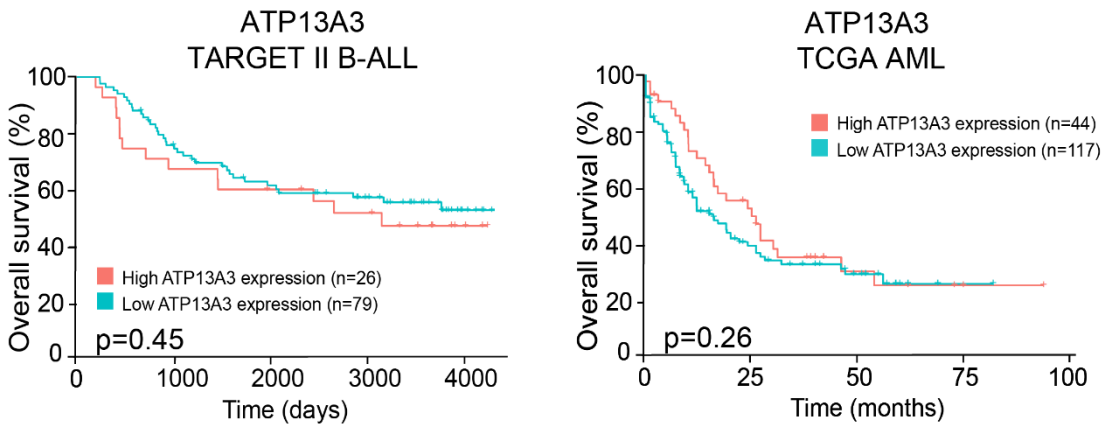

Supplementary Figure 5: ATP13A3 expression levels are not associated with outcome in acute leukaemia. Patients were dichotomised based on upper quartile expression level.

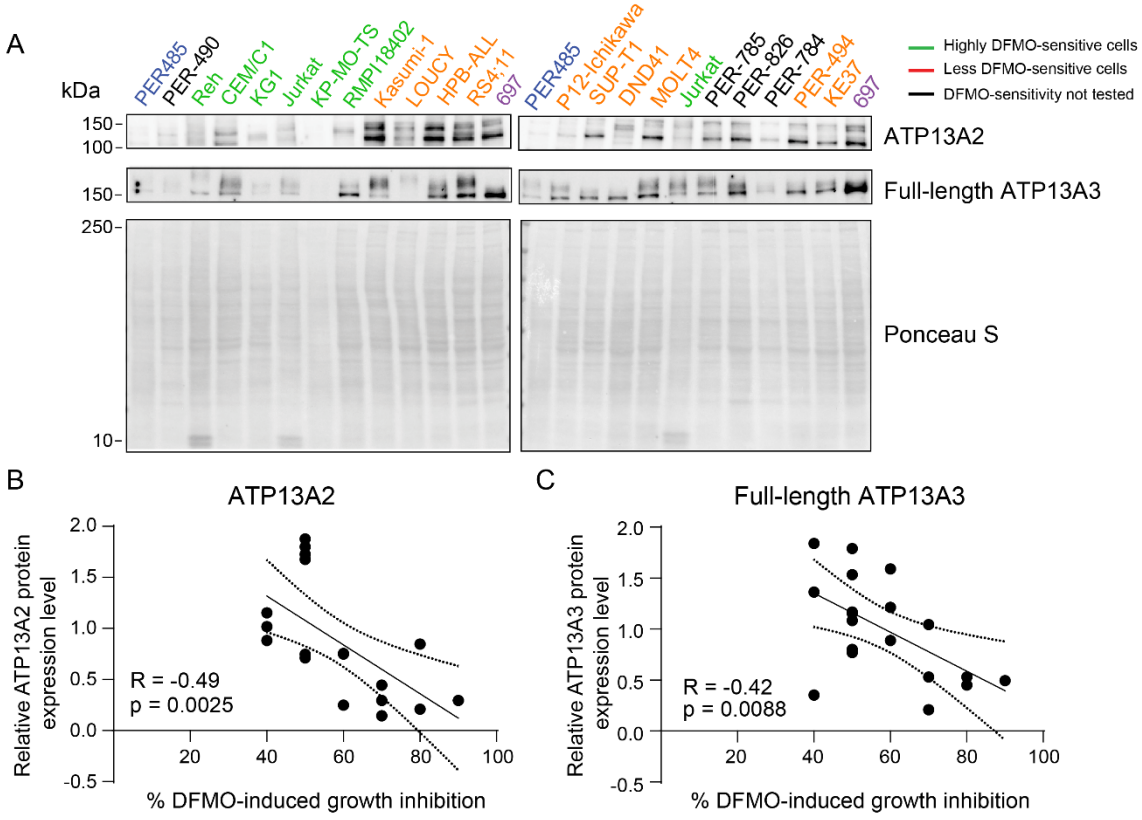

Supplementary Figure 6: Negative correlation between DFMO sensitivity and ATP13A2 and ATP13A3 protein levels in acute leukemia cells. A) Immunoblot for ATP13A2 and ATP13A3 in a panel of acute leukaemia cell lines, representative of two independent experiments. Ponceau staining of whole protein lysate was performed to control for differences in total protein levels loaded and for normalisation purposes. B) Correlation analysis (Pearson) of relative transporter protein ATP13A2 and C) ATP13A3 expression levels and sensitivity to DFMO (represented by % DFMO-induced growth inhibition).

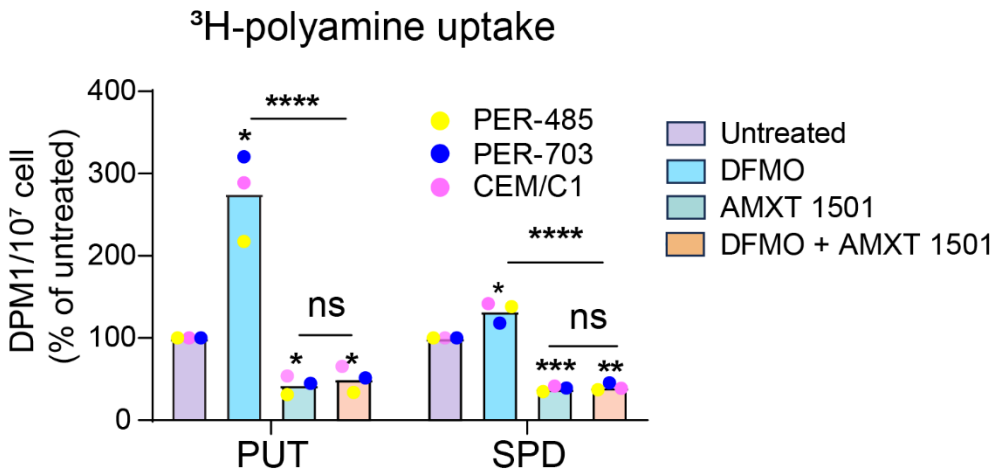

Supplementary Figure 7: **AMXT 1501 abrogates DFMO-induced radiolabelled polyamine uptake in acute leukaemia cells.** ^{3}H-Spermidine Trihydrochloride and ^{3}H-Putrescine Dihydrochloride were added to cells at 0.1-0.2 µCi and incubated at 37 ºC for 90 minutes. Results are represented as mean DPM ± SEM of two independent experiments. DPM1: Disintegrations Per Minute. Asterisks on bars represent P-values calculated by one sample t-test determining whether there is a statistically significant change in the mean uptake in treated versus untreated cells (100%). Stars above lines correspond to P-values calculated by one-way ANOVA. *, p<0.05; **, p<0.01**; P<0.001; ****, P<0.0001.

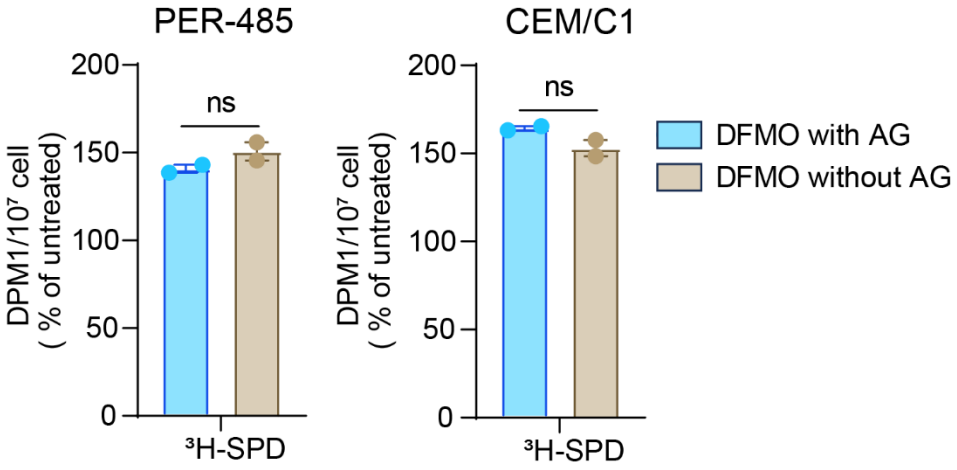

Supplementary Figure 8: Aminoguanidine does not impact radiolabelled spermidine uptake levels in acute leukaemia cells. ^{3}H-Spermidine Trihydrochloride were added to cells at 0.1-0.2 µCi and incubated at 37 ºC for 90 minutes in the presence or absence of 1mM aminoguanidine (AG). Graph depicts % uptake increase in DFMO-treated cells compared to untreated cells (100%) as measured in two independent experiments. DPM1: Disintegrations Per Minute. Mean % uptake increases were compared between groups by Student T-test. ns, not significant.

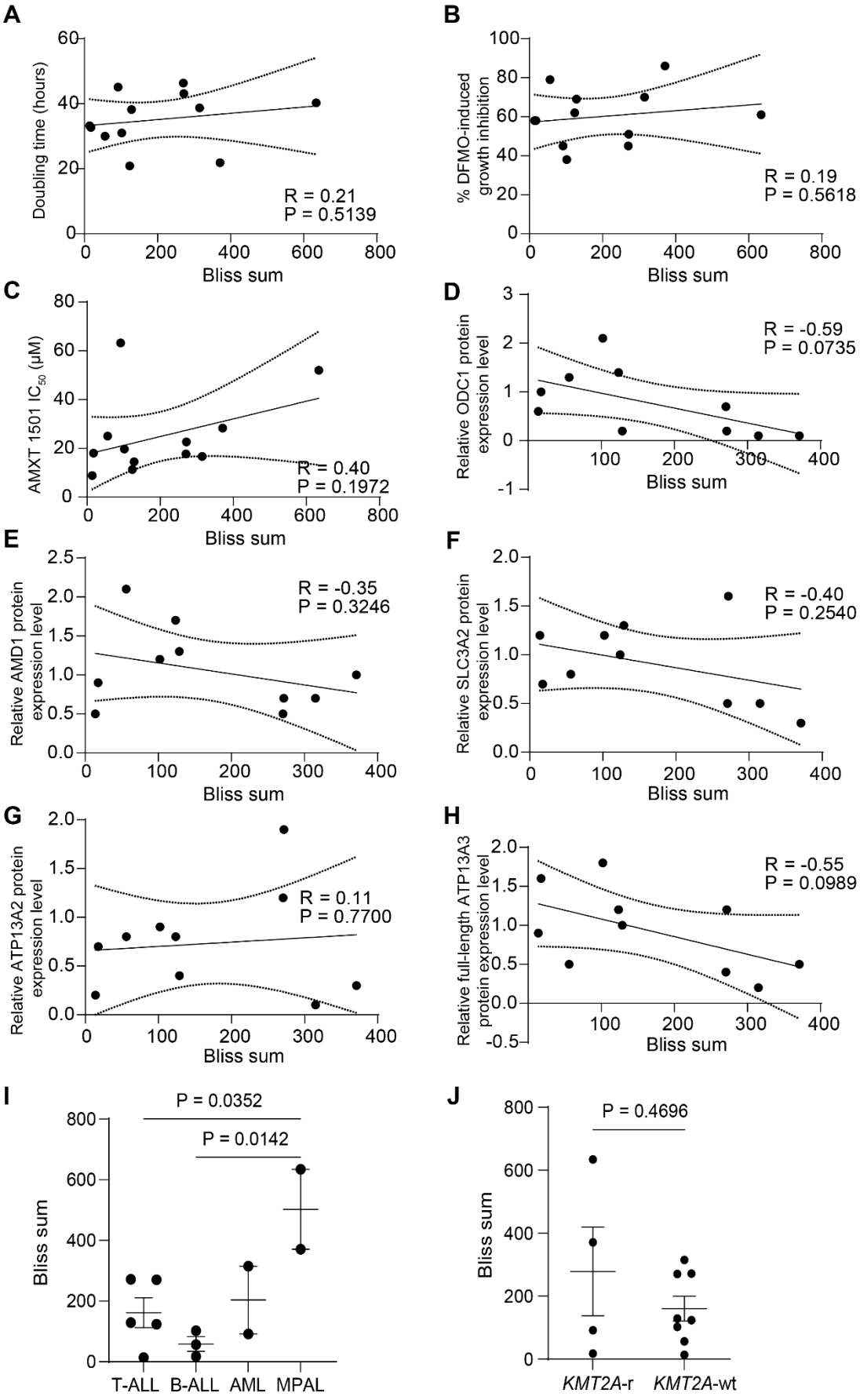
A
Doubling time (hours)
R = 0.21
P = 0.5139
Bliss sum
B
% DFMO-induced growth inhibition
R = 0.19
P = 0.5618
Bliss sum
C
AMXT 1501 IC50 (µM)
R = 0.40
P = 0.1972
Bliss sum
D
Relative ODC1 protein expression level
R = -0.59
P = 0.0735
Bliss sum
E
Relative AMD1 protein expression level
R = -0.35
P = 0.3246
Bliss sum
F
Relative SLC3A2 protein expression level
R = -0.40
P = 0.2540
Bliss sum
G
Relative ATP13A2 protein expression level
R = 0.11
P = 0.7700
Bliss sum
H
Relative full-length ATP13A3 protein expression level
R = -0.55
P = 0.0989
Bliss sum
I
P = 0.0352
P = 0.0142
Bliss sum
T-ALL
B-ALL
AML
MPAL
J
P = 0.4696
Bliss sum
KMT2A-r
KMT2A-wt

Supplementary Figure 9: Determinants of synergy between DFMO and AMXT 1501 in acute leukaemia cells. No statistically significant correlations were observed between DFMO/AMXT 1501 synergy score (Bliss sum) and proliferation rate (A, doubling time), sensitivity to DFMO or AMXT 1501 as single agents (B-C), or protein expression levels of ODC1 (D), AMD1 (E), SLC3A2 (F), ATP13A3 (G) or ATP13A2 (H). (I) Comparison of Bliss sum score between different leukaemia subtypes. One-way ANOVA is used to compare the Bliss sum between groups. (J) Comparison of Bliss sum score between *KMT2A*-r (*KMT2A*-rearranged) and *KMT2A*-wt (*KMT2A* wildtype) leukaemia cells. Student T-test is used to compare the Bliss sum between groups.

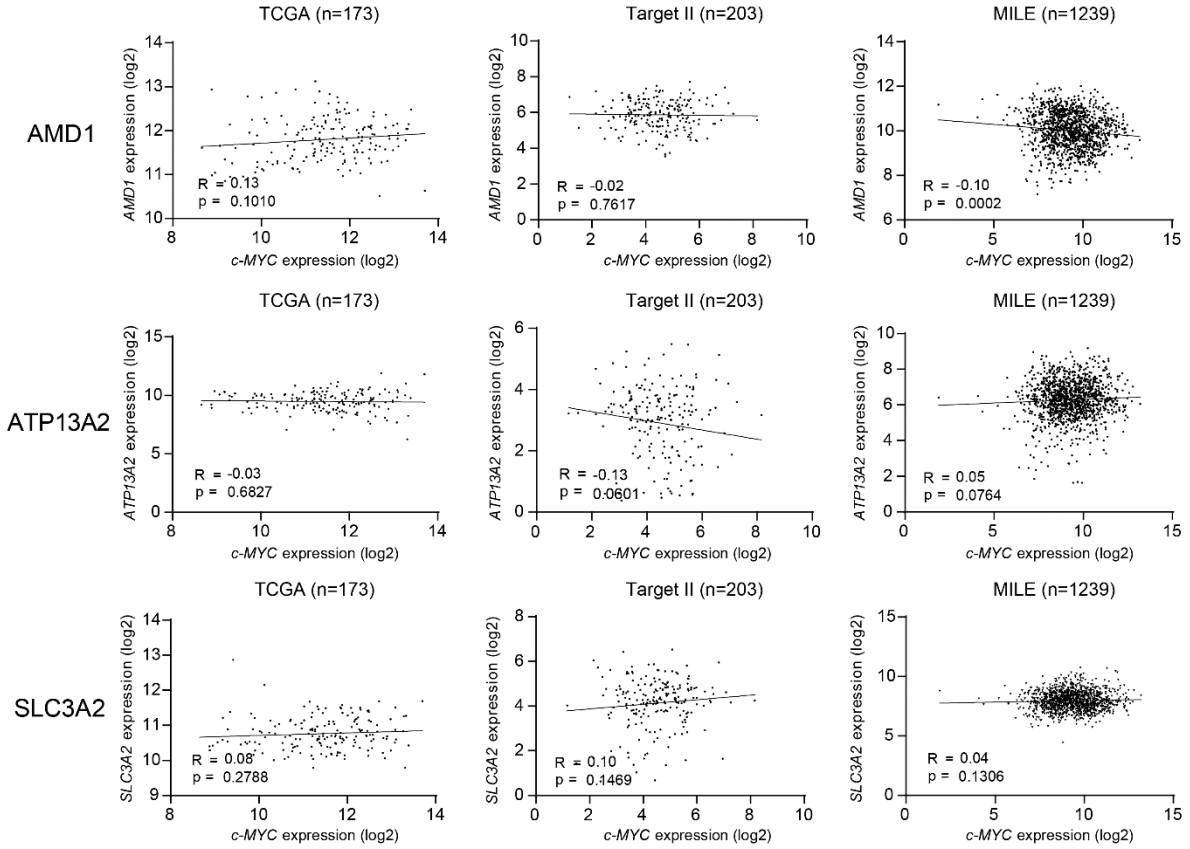

Supplementary Figure 10: No consistent correlations between c-MYC expression and *AMD1*, *ATP13A2* or *SLC3A2* expression levels in patients with leukaemia. Correlation analyses (Pearson) between *c-MYC* mRNA and *AMD1*, *ATP13A2* or *SLC3A2* mRNA expression levels in patients with leukaemia from three databases.

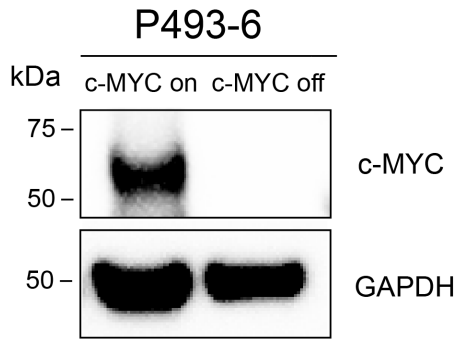

Supplementary Figure 11: **c-MYC expression in P493-6 cells.** P493-6 cells were treated with doxycycline for 72 hrs to silence c-MYC expression (c-MYC off). A blot representative for two independent biological replicates is shown.

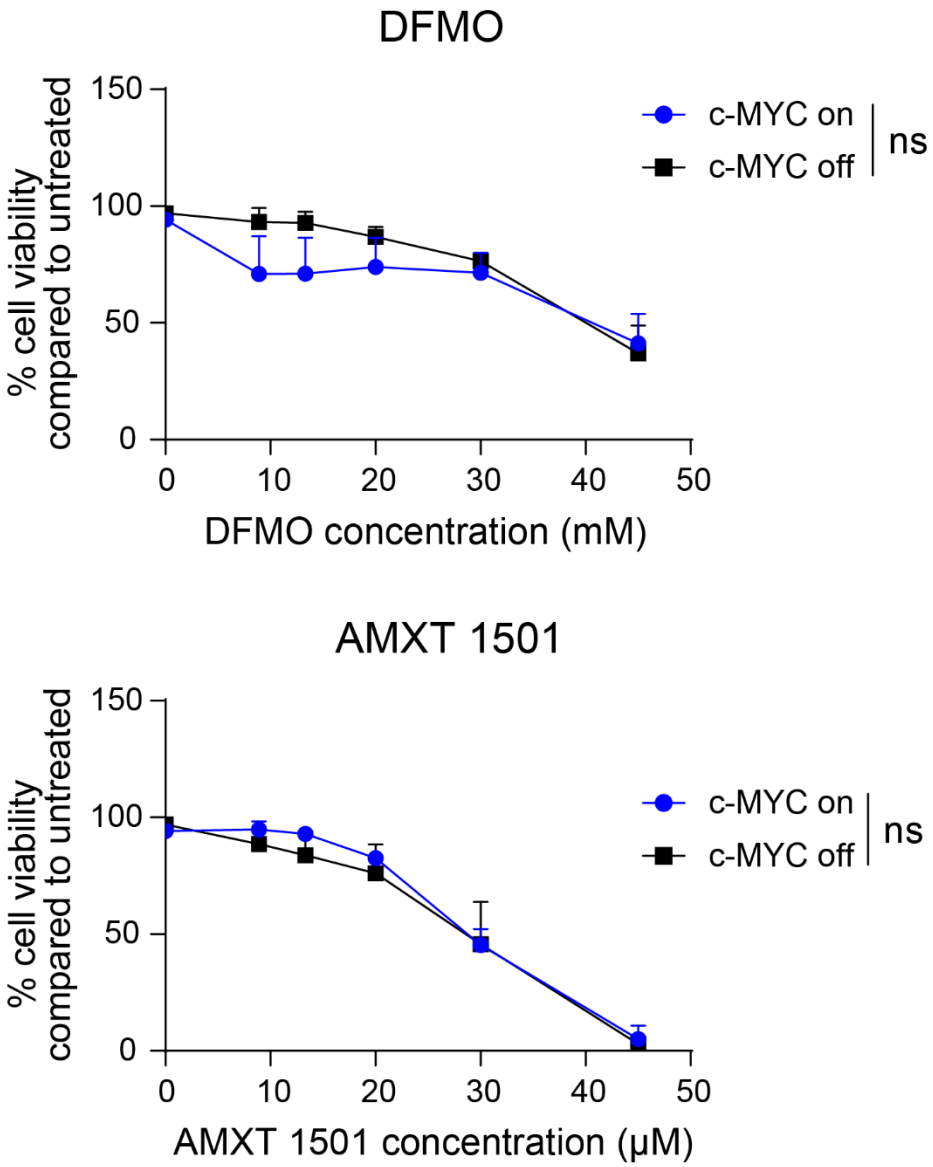

Supplementary Figure 12: *c-MYC* silencing does not significantly impact sensitivity to DFMO or AMXT 1501 as single agents. Single agent dose-response curves obtained in two independently performed 6x6 matrix synergy assays with P493-6 cells measuring resazurin-reduction based viability after 72h drug exposure. ns, not significant.

Supplementary Table 1: Cell lines used in the study

Cell type		Cell line	Disease	Driver	RRID	Supplier
ALL	T-ALL	KE-37	Adult T-ALL	t(8;14)	CVCL_L699	DSMZ
		MOLT-4	Adult T-ALL	t(7;7); 6q-	CVCL_0013	ATCC
		Loucy	Adult T-ALL	t(16;20)	CVCL_1380	ATCC
		P12-Ichikawa	Childhood T-ALL	t(5;14); der(2;9); add(19)	CVCL_1630	DSMZ
		SUP-TI	Childhood T-ALL	t(7;9)	CVCL_1714	ATCC
		RPMI-8402	Childhood T-ALL	t(11;14); del(1)(p32)	CVCL_1667	DSMZ
		HPB-ALL	Childhood T-ALL	TLX3 expression	CVCL_1820	DSMZ
		DND-41	Childhood T-ALL	TLX3 expression	CVCL_2022	DSMZ
		CEM/C1	Childhood T-ALL	t(9;22)	CVCL_3496	ATCC
		Jurkat	Childhood T-ALL	t(9;22)	CVCL_0065	ATCC
	B-ALL	Reh	Childhood B-ALL	t(12;21)	CVCL_1650	ATCC
		697	Childhood B-ALL	t(1;19)	CVCL_0079	DSMZ
		RS4;11	Childhood *KMT2Ar* ALL	t(4;11)	CVCL_0093	ATCC
		SEMK2	Pre-B cell childhood ALL	t(4;11)	CVCL_S906	ATCC
		PER-910	Infant *KMT2A*r ALL	t(9;11)	CVCL_A8JV	Kindly provided by Laurence Cheung and Rishi Kotecha, Telethon Kids Institute, University of Western Australia, WA, Australia
		PER-784	Infant *KMT2A*r ALL	t(2;11)	CVCL_IZ02	
		PER-494	Infant *KMT2A*r ALL	der(4)t(4;11;7)	CVCL_A8JU	
		PER-785	Infant *KMT2A*r ALL	t(4;11)	CVCL_IZ03	
		PER-826	Infant *KMT2A*r ALL	Complex t(11;19)	CVCL_IZ05	
AML		THP-1	Infant *KMT2A*r ALL	t(9;11)	CVCL_0006	Kindly provided by W Jessup, Centre for Vascular Research, NSW, Australia
		MOLM-13	Adult *KMT2Ar* AML	t(9;11)	CVCL_2119	Kindly provided by R D'Andrea, IMVS, SA, Australia
		Kasumi-1	Childhood AML	t(8;21)	CVCL_0589	ATCC
		KP-MO-TS	Childhood AML	CALM-AF10	CVCL_7985	Kindly provided by T Imamura, Kyoto Perfectural University of Medicine, Japan

	KG-1	Adult AML	t(8;21)	CVCL_0374	ATCC
MPAL	PER-485	Infant *KMT2Ar* leukaemia	t(4;11)	CVCL_W984	Kindly provided by provided by Laurence Cheung and Rishi Kotecha, Telethon Kids Institute, University of Western Australia, WA, Australia
	PER-703	Infant *KMT2Ar* leukaemia	t(1;11)	CVCL_IY99	
lymphoblastoid cell line	P493-6	B-lymphoblastoid	c-MYC	CVCL_6783	DSMZ
Non-malignant cell	MRC-5	Non-malignant lung fibroblast	-	CVCL_0440	ATCC

ALL: acute lymphoblastic leukaemia; B-ALL: B-cell acute lymphoblastic leukaemia; T-ALL: T-cell acute lymphoblastic leukaemia; AML: acute myeloid leukaemia; MPAL: mixed-phenotype acute leukaemia; *KMT2A*r: *KMT2A*-rearranged.

Supplementary Table 2: Complete summary of *in vivo* responses of DFMO and AMXT 1501 in leukaemia animal models

Xenograft	Treatment Group	Animal Counts/Status					EFS Evaluation				
		N[1]	Nd[2]	Nx[3]	Na[4]	Nev[5]	KM med[6]	EFS T - C[7]	EFS T/C[8]	P-value[9]	P-value[10]
PER-485	Vehicle (D-mannitol)	6	0	0	6	6	15.0				
	1% DFMO	6	0	0	6	6	18.0	3.0	1.20	0.0443	0.0033
	1.25mg/kg AMXT 1501	6	0	0	6	6	18.0	3.0	1.20	0.0347	0.0074
	1% DFMO + 1.25mg/kg AMXT 1501	6	0	0	6	6	22.0	7.0	1.47	0.0012	
	AraC 25mg/kg + Daunorubicin 0.625mg/kg	6	0	0	6	6	16.5	1.5	1.10	0.5017	
MLL-3	Vehicle (D-mannitol)	7	0	0	7	7	10.1				
	1% DFMO	7	0	0	7	7	10.4	0.3	1.03	0.638	0.0031
	1.25mg/kg AMXT 1501	7	0	0	7	7	12.8	2.8	1.27	0.0004	0.7504
	1% DFMO + 1.25mg/kg AMXT 1501	7	0	0	7	7	13.2	3.2	1.31	0.0017	

[1]N = total number of mice entering experiment

[2]Nd = number of mice experiencing toxic death

[3]Nx = number of additional mice excluded from analysis

[4]Na = number of mice in analysis

[5]Nev = number of events, defined as $hCD45^+$ cells ≥ 50% or mouse becomes moribund

[6]KM med = Kaplan-Meier estimate of median time-to-event (days)

[7]EFS T – C = Leukemia Growth Delay (LGD) = difference in median time-to-event (days) between T and C groups

[8]EFS T/ C = relative difference in median time-to-event (days) between T and C groups

[9]P-value comparing EFS (treatment group) to EFS (vehicle-treated group), computed using Gehan-Wilcoxon test

[10]P-value comparing EFS (combination treatment group) to EFS (single agent-treated group), computed using Gehan-Wilcoxon test